

UNIVERSITÀ DEGLI STUDI DI SALERNO



DIPARTIMENTO DI INGEGNERIA
DELL'INFORMAZIONE ED ELETTRICA E
MATEMATICA APPLICATA

DOTTORATO DI RICERCA IN INFORMATICA E INGEGNERIA
DELL'INFORMAZIONE
XV CICLO - NUOVA SERIE

Vehicular Traffic on Networks: Comparison among Solutions Modeling Vertex Flow

CANDIDATO: **Guarino Giuseppe**

COORDINATORE: **Chiar.mo Prof. Alfredo De Santis**

TUTOR: **Chiar.mo Prof. Ciro D'Apice**

CO-TUTOR: **Prof.ssa Rosanna Manzo**

ANNO ACCADEMICO 2015-2016

Contents

1	Introduction	1
2	Macroscopic Traffic Models	5
2.1	Variables regulating vehicular traffic	6
2.1.1	Velocity	7
2.1.2	Flux	7
2.1.3	Density	8
2.1.4	Relation among velocity, flux and density . .	9
2.2	Conservation law for vehicular traffic	10
2.3	Lighthill-Whitham-Richards Model	12
2.3.1	Fundamental Diagrams	14
2.3.2	Riemann Problem	17
2.3.3	Shock and rarefactions development in traf- fic models	20
2.3.4	Lighthill-Whitham-Richards Model with Vis- cosity	22
2.4	Payne-Witham Model	24
2.5	Aw-Rascle Model	26
2.6	Zhang Model	27
2.7	Third order Models	29
2.8	Multilane Model	29
3	Fluid-dynamic model for vehicular traffic networks	33
3.1	Assumptions	33
3.2	Solution of Riemann problem for specific cases . . .	38
3.3	Alternative Riemann Solver at Intersections	42

3.3.1	The Riemann Solver (R1-1)	46
3.3.2	The Riemann Solver (R1-2)	47
3.3.3	The Riemann Solver (R1-3)	47
3.3.4	The Riemann Solver (R1-4)	49
3.3.5	The Riemann Solver (R2-1)	49
3.3.6	The Riemann Solver (R2-2)	50
3.3.7	The Riemann Solver (R2-3)	51
3.3.8	The Riemann Solver (R2-4)	51
3.4	Formulation of the Linear Programming Model for Riemann Solver	51
3.4.1	Assumptions for Alternative Riemann Solvers	53
4	Numerical Schemes	55
4.1	Approximations of non-linear hyperbolic problems .	55
4.1.1	Approximation finite difference	55
4.1.2	Approximation with discontinuous finite el- ements	58
4.2	Numerical methods for vehicular traffic networks . .	60
4.2.1	Godunov method	61
5	Experimentation and Numerical Results	67
5.1	Operating Specifications	67
5.1.1	Configuration parameters	67
5.1.2	Input data	69
5.1.3	Output data	71
5.2	Case Study	71
5.3	Experimentation results	75
6	Conclusions	89

List of Figures

2.1	Traffic density is inverse of spacing	8
2.2	Constant flow of vehicles	9
2.3	Distance traveled by a car in τ hours	9
2.4	Incoming and outgoing cars within a road interval .	10
2.5	$v = v(\rho)$ state	13
2.6	Flow diagram as a function of density	14
2.7	Velocity function and fundamental diagram for (1.9)	15
2.8	Velocity function and fundamental diagram for (1.10)	16
2.9	Velocity function and fundamental diagram for (1.11)	17
2.10	ρ^+ and ρ^- state	18
2.11	The solution to the Riemann problem when $\rho^- < \rho^+$	19
2.12	The solution to the Riemann problem when $\rho^- > \rho^+$	19
2.13	Traffic density due extremely long phase	20
2.14	Rarefaction wave	21
2.15	Density as result of stopped vehicular traffic	21
2.16	The initial configuration ρ_0	23
2.17	The functions w_1 and w_2 for the multilane model .	31
3.1	Example of simple road network	34
3.2	Example of 2×1 Intersection	39
3.3	2×1 Intersection: Case 1 and 2	40
3.4	Example of 2×2 Intersection	41
3.5	2×2 Intersection - Final fluxes region	42
4.1	Grid	56
5.1	Road Network Graph	68

5.2	Distribution coefficients	70
5.3	Priority	70
5.4	Example of Simulator Configuration	71
5.5	OSM Map of Salerno city	72
5.6	Case study - Road network	72
5.7	Intersection B - Incoming Road ID7	77
5.8	Intersection B - Outgoing Road ID3	78
5.9	Intersection B - Outgoing Road ID5	78
5.10	Intersection A - Incoming Road ID2	79
5.11	Intersection A - Incoming Road ID5	80
5.12	Intersection A - Outgoing Road ID6	81
5.13	Intersection A - Incoming Road ID2 - RS 2 Simulation	83
5.14	Intersection A - Incoming Road ID5 - RS 2 Simulation	84
5.15	Intersection A - Incoming Road ID2 - RS 2 Simulation with different priorities	85
5.16	Intersection A - Incoming Road ID5 - RS 2 Simulation with different priorities	86
5.17	Intersection A - Outgoing Road ID6 - RS 2 Simulation with different priorities	86
5.18	Intersection C - Incoming Road ID7 - RS 2 Simulation with $q_2=0.3$ and $q_5=0.7$	87

List of Tables

2.1	Payne-Whitham Model Terms	24
5.1	Case study - List of roads	73
5.2	Case study - List of intersections	74

Chapter 1

Introduction

In recent years, the analysis of issues associated with road traffic within urban and suburban areas has taken a leading role in trying to implement efficient plans of transport regulations by taking advantage of the available infrastructure. The increasing popularity of vehicles, the decentralization of industrial areas and towns and a public transport service often lacking resulted in a sharp increase in the overall demand for transport, with a relative traffic increase. Consequently, the occurrence frequency of slowdowns phenomena and the strong congestion has greatly multiplied and caused a series of inconveniences and poor services for citizens such as the increased risk of accidents and air and noise pollution (just think of the waste gas of cars and noise of the engines running). In order to solve the problem of urban mobility, it is possible to act with a rational management of infrastructure and a road-artery planning program using simulators able to identify critical points in the design phase and evaluate the correctness of the proposed interventions. Therefore, it is important to use mathematical models to predict the evolution of the traffic starting from the knowledge of quantities such as cars density at a given time instant. Traffic prediction models can be classified in microscopic and macroscopic according to detailed level used. The microscopic models analyze the behavior of each single vehicle, while the macroscopic ones consider situations that arise from the interaction of many particles

based on concepts of the fluid dynamics.

The first macroscopic fluid dynamic model for single road dates back to the years 50's when J. Lighthill and G. Whitham, two experts of fluid dynamics (and independently P. Richards), realized that the equations describing the flux of water (partial differential equations known as Euler equations or Navier-Stokes equations, which express the conservation of mass, momentum and energy) could be able to also capture the dynamics of the traffic flux. The basic idea is to consider a wide spatial scale, which is equivalent to observing the phenomenon "very far", in order to consider vehicles as small particles (with no distinction between trucks, cars, buses, etc.) and to assume that the density has a continuous distribution. In any case, it is reasonable to assume the conservation of the number of vehicles in a road section without outputs or inputs, thus arriving at a conservation law that is a particular partial differential equation, where the variable is a quantity that is conserved, i.e. an amount that can be neither created nor destroyed.

Although the first model based on the conservation laws was applied to traffic on single road, the fluid dynamic models are a wide range of application; in fact, they may be used to describe the evolution of the traffic of road networks of large towns or highways of great states, streams of data on telecommunications networks, fluxes of goods on production chains, gas networks, power grids, blood flux, etc. In other words, these models are capable of describing real systems in which something is preserved: the average number of vehicles along a road, of packets network on Internet, the number of goods produced in a production chain, etc.

The aim of the Thesis is to review macroscopic fluid dynamic models dealing with traffic flow on road networks and to propose new solutions for the dynamics at intersections based on the integration of optimization criteria about the vehicular flow and rules for the distribution of traffic.

In detail, the Thesis is organized as follows.

In **Chapter 2**, we firstly introduce the physical variables that regulate road traffic and the relation that links them with each other, and then some fluid dynamic macroscopic models for traf-

fic on a single road are presented. We start describing in detail the first order model of Lighthill, Whitham and Richards (LWR model). Then we pass to the second order models (i.e. systems of two equations) proposed by Payne and Whitham and by Aw and Rascle. Various other more complex models are included, e.g. Zhang, third order, multi-lane.

In **Chapter 3** we describe the road network model based on the conservation laws. For the ends that do not touch an intersection and are not infinite, initial conditions are assigned and the corresponding boundary value problems are solved. In order to complete the model, it is necessary to assign the dynamics at intersections. A possible requirement is the conservation of the density flux through intersections, expressed by the equality between incoming and outgoing fluxes. However, in some cases the conservation is not strictly necessary from the modeling point of view. This may be a modeling choice or it may be due to absorption at vertices, e.g. for the presence of queues. In any case, the only conservation of density at intersections is not sufficient to describe uniquely the dynamics. Usually, it is possible to assign some traffic distribution rules from incoming arcs to outgoing ones, together with flux (or other functional) maximization. In some cases, additional rules must be used. For instance, for an intersection of a road network with two incoming and one outgoing roads, one has to describe the right of way of the two incoming roads. In general, the dynamics at intersections can be described by giving the solution to Riemann problems, which are Cauchy problems with constant initial data on each road. We start by giving the definition of Riemann Solver (RS). Roughly speaking, a RS is a map assigning the solutions to Riemann problems as functions of their initial data. Then, we consider new models for the simple case of a single conservation law. Starting from two basic RS, we consider four additional rules, justified by modeling choices. Finally, we determine which rules effectively individuate a RS and which of the latter possess good properties to generate a well-posed theory.

Chapter 4 is dedicated entirely to numerical schemes used for

the discretization of the conservation law and the solution of the dynamic at intersections. In detail, Godunov scheme, used for the determination of density values for road sections in different time instants starting from the initial density value of each road on the analyzed road network, will be described.

Chapter 5 describes numerical results about experimentation of some of the defined models based on Riemann Solver solutions that are implemented within a road traffic simulator prototype by reproducing the behaviour of vehicular densities on a road network with appropriate dynamics at intersections. Then, we compare these results in order to prove the correctness of each model, and to point out the most suitable solution that better models the specific dynamics at intersections with the aim of optimizing traffic flow.

Finally, **Chapter 6** presents some conclusions about experimentation of models based on Riemann Solver by suggesting how numerical results of the simulation can be understood for predicting risks on roads and can be useful for planning maintenance of road networks.

Chapter 2

Macroscopic Traffic Models

Main goal of macroscopic traffic models is the description of the evolution of vehicle positions basing on macroscopic variables like density and average speed of vehicles. Vehicular traffic can be considered as a flowing rider; for this reason, it is quite natural to associate the traffic flux to flow of a fluid and treat it accordingly. The first fluid-dynamic model for single road dates back to the 50s by J. Lighthill, Whitham [29] and Richards [25] and it is based on conservation of the average number of cars in a road segment without entry and exit ways. From a mathematical point of view, fluid-dynamic models are represented as equations or hyperbolic and nonlinear conservation laws systems, whose solutions are generally discontinuous and they must be analyzed within the scope of entropic weak solutions. Another example of model, described by two equations, were proposed by Payne (1971) [22] [23] and Whitham (1974) [28] but, unfortunately, it was proved by Daganzo [9] that these models are not good to describe traffic flux. His theory was based on the demonstration that cars could exhibit negative speed. Finally, Aw and Rascle (2000) [1] overcome Daganzo' observations by proposing a second order model that became a starting point for a lot of other traffic models.

Although there is a copious literature on traffic flux models for single road, in one or more lanes, only few contributions were concerned to the case of traffic networks. In fact, Holden-Risebro

(1995) and Piccoli et al. (2005) obtained first results about traffic networks [14]. Existence and uniqueness of solutions for traffic networks with simple intersections (i.e. two incoming and two outgoing roads) was given by considering a method based on Riemann problems at intersections (Cauchy problems with constant initial data on each incoming and outgoing road) and a suitable version of Wave Front-Tracking algorithm by Bressan.

Main advantage of fluid-dynamic approach is that by using a parsimonious number of parameters, models are capable of describing evolution of network load at each time instant and disclosing some phenomena such as formation of queues and their propagation as a result of sudden changes or special circumstances. In addition, the theory allows the development of efficient numeric schemas also for large networks, thanks to the modeling of the flux at the intersections in a simple and computationally way, which makes use of linear programming problems.

In this section, we first introduce variables regulating vehicular traffic on networks used within macroscopic traffic models and then we describe some of these models proposed in literature.

2.1 Variables regulating vehicular traffic

Analogy with fluids of fluid-dynamic approach leads us to focus on some physical parameters such as flux, concentration (in terms of spatial density) and speed.

Vehicular traffic can be modeled as a mono-dimensional incompressible fluid under the following hypothesis:

1. Traffic flux is preserved and is regulated by a conservation law.
2. There is a correspondence between speed and density and between flux and density that results into an equation of state.

2.1.1 Velocity

Velocity (or **speed**) of an object is defined as total space distance divided by used time; about vehicular traffic, velocity v_i of each car is given by relation

$$v_i(t) = \frac{dx_i(t)}{dt},$$

where $x_i(t)$ is car position at time t .

In many situations, number of cars is so high that it is difficult to keep track of each of them; therefore, instead of measuring speed of every single car, for each point in the space and for each time instant a speed range $v(x, t)$ is considered as

$$v(x_i(t), t) = v_i(t).$$

In this way overtaking among cars is not considered because, in point of overtaking, the speed would assume different values at the same instant.

2.1.2 Flux

Traffic **flux** (or **flow**) is defined as the average number of cars per unit of time (for example, one hour), measured by a fixed observer in a given position and, then, it is function of the position x and time t , $f(x, t)$.

Selection of the time interval for measuring the flux is crucial. It is assumed that there is a measuring interval which is:

- long enough, so that during this interval a high number of cars passes through observation point (thus eliminating sudden fluctuations);
- small enough, so that variations within the traffic flux is not softened by averaging about a period of time too long.

2.1.3 Density

Traffic **density** is the number of cars (per lane) for spatial measurement unit (for example a kilometer) where *car* term means any vehicle.

Assuming that all cars have length L and distance between two of them is d (see Figure 2.1), the density is defined as

$$\rho = \frac{1}{L+d}.$$

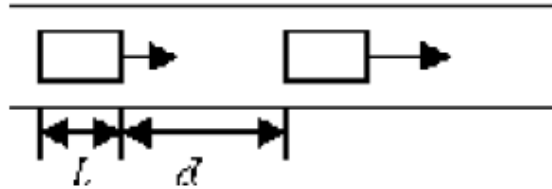


Figure 2.1 Traffic density is inverse of spacing

Even for the density, the length of interval in which the cars are counted must be chosen so as to be large enough in order to be able to contain a high number of them and small enough in order not to lose local densities (changes of density).

2.1.4 Relation among velocity, flux and density

There is a relation among velocity, flux and density quantities. We consider one of the most simple traffic situations. We suppose that, on a road, the traffic is moving at a constant velocity v_0 . Since each car moves with the same velocity, the distance among vehicles is constant and, for this reason, the traffic density is constant, $\rho = \rho_0$ (see Figure 2.2).

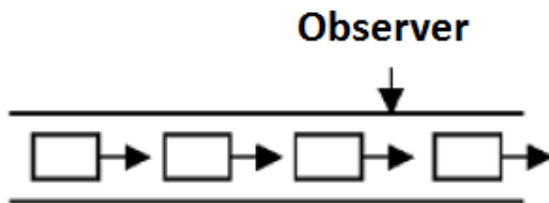


Figure 2.2 Constant flow of vehicles

We calculate traffic flux. Since the velocity is constant, distance traveled is given by velocity multiplied time. In τ hours, each car has traveled the distance $v_0\tau$; for this reason, the number of cars observed in τ hours is given by the number of cars within interval of length $v_0\tau$ (see Figure 2.3).

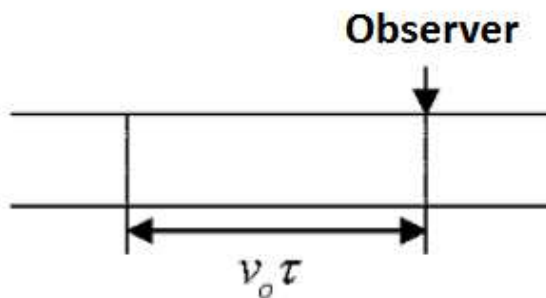


Figure 2.3 Distance traveled by a car in τ hours

Since ρ_0 is the number of cars per kilometer, $\rho_0 v_0 \tau$ is the number of cars observed in τ hours.

Traffic flux is given by

$$f = \rho_0 v_0.$$

Although it was derived for a simplified case, in general the fundamental law is valid:

$$f(x, t) = \rho(x, t)v(x, t),$$

that links the flux to the density and velocity.

2.2 Conservation law for vehicular traffic

We consider a road interval with ends $x = a$ and $x = b$ (see Figure 2.4).

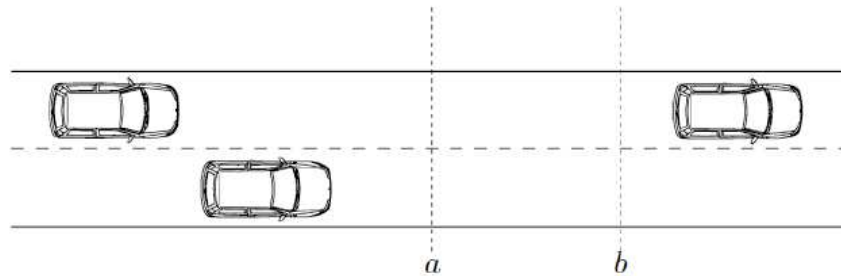


Figure 2.4 Incoming and outgoing cars within a road interval

Assuming that the density $\rho(x, t)$ is continuous, the number of cars N is given by the following integral:

$$N = \int_a^b \rho(x, t) dx. \quad (1.1)$$

So, the number of cars between $x = a$ and $x = b$ is constant. Variation of vehicular number per time unit is given by difference between the number of crossings per unit of time within $x = a$ (movements to the right) and the number of crossings (movements to the left) within $x = b$, that is:

$$\frac{dN}{dt} = f(a, t) - f(b, t), \quad (1.2)$$

where the number of cars per time unit is the flux $f(x, t)$.

By combining equations (1.1) and (1.2) we obtain:

$$\frac{d}{dt} \int_a^b \rho(x, t) dx = f(a, t) - f(b, t). \quad (1.3)$$

This equation is called **integral conservation law** and specifies that changes in the number of cars are essentially due to the flux through towards the ends of considered interval.

Equation (1.3) can be conveyed as *local conservation law* that is valid within each position of the road and, in this case, the ends of the road interval $x = a$ and $x = b$ can be considered additional independent variables. Total derivative according to Equation (1.3) must be replaced by a partial derivative:

$$\frac{\partial}{\partial t} \int_a^b \rho(x, t) dx = f(a, t) - f(b, t).$$

We observe that under suitable regularity assumptions for the function ρ :

$$f(a, t) - f(b, t) = - \int_a^b \frac{\partial}{\partial t} [\rho(x, t)] dx,$$

we have:

$$\int_a^b \left[\frac{\partial}{\partial t} \rho(x, t) + \frac{\partial}{\partial x} f(x, t) \right] dx = 0. \quad (1.4)$$

Given the arbitrariness of the limits of integration it follows that:

$$\frac{\partial \rho}{\partial t} + \frac{\partial f}{\partial x} = 0.$$

Being $f = \rho v$ it is possible to write the conservation law in the following form:

$$\frac{\partial \rho}{\partial t} + \frac{\partial(\rho v)}{\partial x} = 0. \quad (1.5)$$

2.3 Lighthill-Whitham-Richards Model

The fluid-dynamic model for single road (**LWR model**) is based on two relations already seen:

$$f = \rho v \quad (1.6)$$

$$\frac{\partial \rho}{\partial t} + \frac{\partial f}{\partial x} = 0, \quad (1.7)$$

that are valid for macroscopic variables of traffic as well as for fluid but they are not enough to characterize the traffic flux.

If the velocity is known, Equation (1.5) is a partial differential equation that allows to predict future traffic density from well-known initial one (**Cauchy problem**). In order to solve this equation it is important to analyze velocity field.

In the mid-50s Lighthill Whitham and Richards developed a model based on relations (1.6) and (1.7), by assuming that the velocity depends only by density in each point, that is $v = v\rho$.

Under this hypothesis, the flux f is function only of density

$$f = f(\rho).$$

According to this model, if the traffic density is very low cars will travel at maximum speed v_{\max} :

$$v(0) = v_{\max}.$$

With increasing of density the presence of other cars will slow car speed, thus

$$\frac{dv}{d\rho} = v'(\rho) \leq 0.$$

At maximum density ρ_{\max} we have

$$v(\rho_{\max}) = 0.$$

Notice that cars stop due to dense traffic conditions before they crash. Then, $\rho_{\max} < \frac{1}{L}$, where L is the average length of a vehicle. One possible curve $v = v(\rho)$ is shown in Figure 2.5.

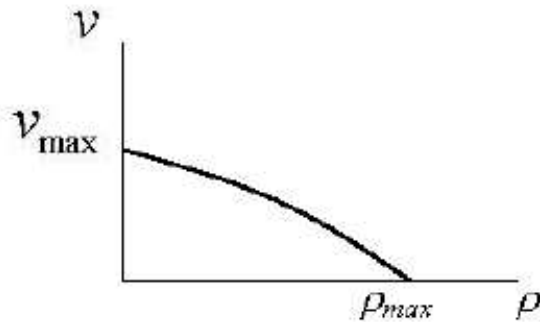


Figure 2.5 $v = v(\rho)$ state

About $v = v(\rho)$, there are some implicit assumptions:

- equal density, the speed of different drivers is the same. Therefore, irregular behavior of individual drivers is ignored. It would be more realistic to introduce a stochastic model in which it is expected that at a certain density a percentage of drivers travels at a given speed and others at slightly different speeds;
- high-speed car that is approaching to a slower traffic segment must itself slow down. The model does not provide more overtaking lanes on a single road;
- model does not consider finite time of reaction of drivers nor finite response time required by motor to change speed (acceleration and deceleration).

The flux expressed as $f = \rho v(\rho)$ has some general properties. It is null if there is no traffic ($\rho = 0$) or if the traffic does not move ($v = 0$ and $\rho = \rho_{\max}$); contrariwise, for $0 < \rho < \rho_{\max}$ traffic flux must be positive.

Figure 2.6 shows a flux state as a function of density. Maximum traffic flux is called **capacity** of road.

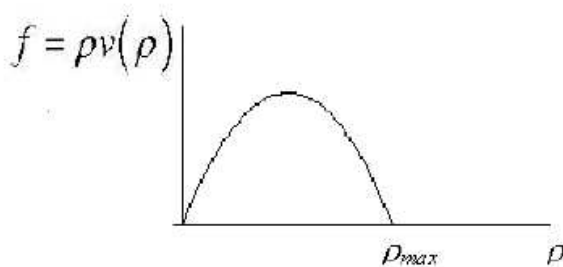


Figure 2.6 Flow diagram as a function of density

Because

$$\frac{\partial}{\partial x} f(\rho) = \frac{df}{d\rho} \frac{\partial \rho}{\partial x},$$

we can write the conservation law as

$$\frac{\partial}{\partial t} \rho(x, t) + \frac{d}{d\rho} f(\rho(x, t)) \cdot \frac{\partial}{\partial x} \rho(x, t) = \frac{\partial}{\partial t} \rho(x, t) + C(\rho(x, t)) \cdot \frac{\partial}{\partial x} \rho(x, t) = 0, \quad (1.8)$$

where $C(\rho) = f'(\rho)$.

Equation (1.8) is a partial differential equation derivative almost linear of hyperbolic type and can be resolved with appropriate methods.

2.3.1 Fundamental Diagrams

The main assumption for Lighthill-Whitham-Richards Model is that the average velocity v depends only by the density of the cars. One reasonable property of v is that v is a decreasing function of the density. The law that returns the flux as function of the density is called *fundamental diagram* [14].

Some different fundamental diagrams are described below. For each diagram the velocity function $v = v(\rho)$ is assigned, thus the flux is simply calculated by multiplying the density ρ .

A first, and more simple, fundamental diagram considered by **Greenshield** is generated by setting v to be a linear function of the density (see Figure 2.7) [14], i.e.

$$v(\rho) = v_{\max}\left(1 - \frac{\rho}{\rho_{\max}}\right). \quad (1.9)$$

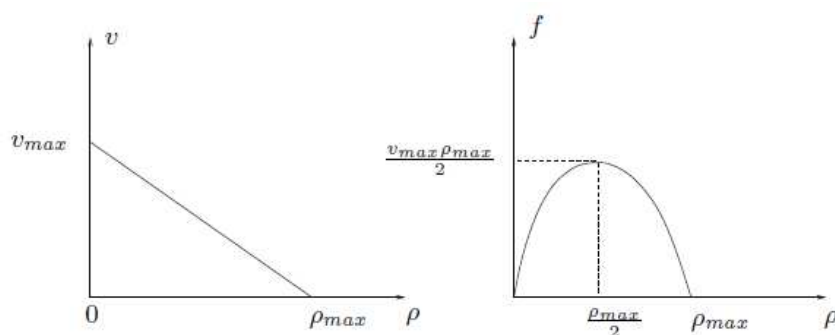


Figure 2.7 Velocity function and fundamental diagram for (1.9)

It is based on three main considerations:

1. the velocity decreases with increasing density, which corresponds to $\frac{dv}{d\rho} \leq 0$;
2. the velocity is proportional to a maximum velocity v_{\max} so that in low density correspondence this is the vehicular velocity;
3. the velocity is directly proportional to the difference $\rho_{\max} - \rho$, where ρ_{\max} is the maximum density.

A second fundamental diagram was considered by **Greenberg** and was supported by experimental data from the Lincoln Tunnel in New York city. He set the velocity function as

$$v(\rho) = v_0 \log\left(\frac{\rho_{\max}}{\rho}\right), \quad (1.10)$$

where v_0 is a positive constant. In this case $v(\rho_{\max}) = 0$, while v is unbounded when $\rho \rightarrow 0^+$, as shown in Figure 2.8 [14].

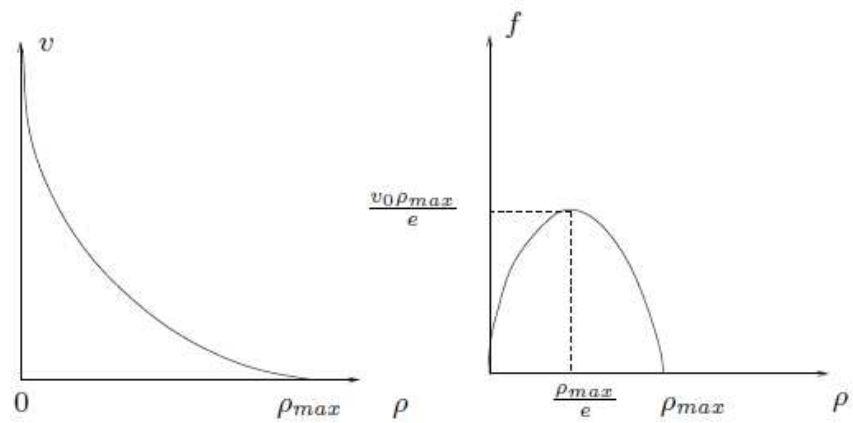


Figure 2.8 Velocity function and fundamental diagram for (1.10)

A third fundamental diagram is given by the **Underwood** model, whose velocity function is

$$v(\rho) = v_{\max} e^{-\frac{\rho}{\rho_{\max}}}. \quad (1.11)$$

This model assumes that the average velocity is non zero even if the density is the maximal possible, as shown in Figure 2.9 [14].

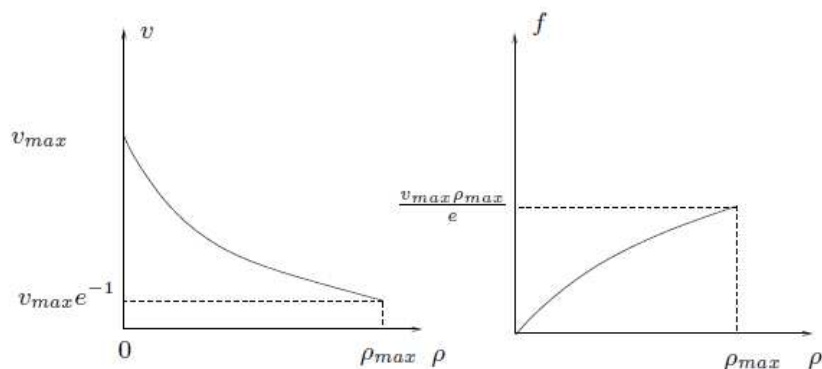


Figure 2.9 Velocity function and fundamental diagram for (1.11)

2.3.2 Riemann Problem

A recurring phenomenon in the dynamics of a fluid is the development of discontinuity surfaces, such as sources of shock and rarefaction waves, through which the properties of the fluid such as pressure, density, and velocity change according to a strictly fast mode.

The study of the dynamics of these surfaces has a long history, and a fundamental contribution was offered by Riemann who more than a hundred years ago calculated what it happens to a perfect fluid which has, at a given initial instant, planar discontinuities in the fluid variables.

This problem, known as the **Riemann problem**, provides that there are different solutions, corresponding to the combinations in which the shocks and rarefaction waves can propagate along opposite direction in the unperturbed fluid.

Consider a conservation law

$$\rho_t + f(\rho)_x = 0,$$

with initial condition

$$\rho(x, 0) = \begin{cases} \rho^- & \text{if } x \leq 0 \\ \rho^+ & \text{if } x > 0 \end{cases}$$

This is a Cauchy problem that has a *Heavyside* function as an initial condition. Heavyside step function, also called function at single step, is a discontinuous function which is zero for negative arguments and one for positive ones.

ρ^+ and ρ^- values are respectively called *right state* and *left state* (see Figure 2.10).

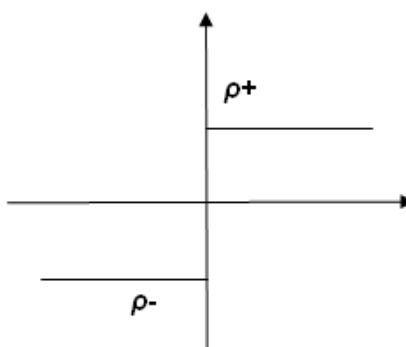


Figure 2.10 ρ^+ and ρ^- state

Such Riemann problem is very important because it is the first step in order to define the solutions for Cauchy problem.

Riemann problem can be easily solved if we make some simplifying assumptions about the flux function. In particular, let $f : \mathbb{R} \rightarrow \mathbb{R}$ of class C^2 strictly convex, that is

$$f(\alpha\rho_1 + (1 - \alpha)\rho_2) \leq \alpha f(\rho_1) + (1 - \alpha)f(\rho_2),$$

$\forall \rho_1, \rho_2 \in \mathbb{R}, \forall \alpha \in]0, 1[$. We denote by g the inverse function of f . Under this assumption, it is possible to prove that if $\rho^- > \rho^+$, Riemann problem has as solution

$$\rho(x, t) = \begin{cases} \rho^-, & \text{if } x < \lambda t \\ \rho^+ & \text{if } x \geq \lambda t \end{cases}$$

where λ satisfies Rankine-Hugoniot condition, that is

$$\lambda = \frac{f(\rho^+) - f(\rho^-)}{\rho^+ - \rho^-}.$$

The wave velocity is positive if $f(\rho^+) > f(\rho^-)$, while it is negative if $f(\rho^+) < f(\rho^-)$ (see Figure 2.11).

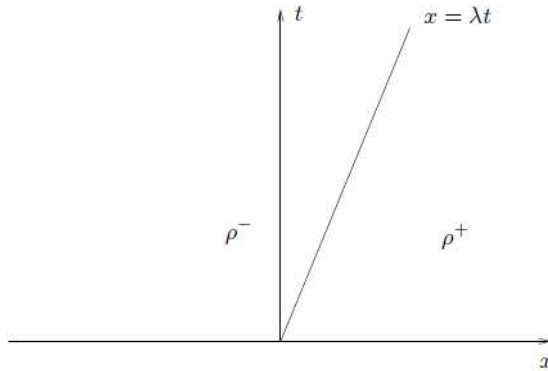


Figure 2.11 The solution to the Riemann problem when $\rho^- < \rho^+$

Otherwise, if $\rho^- > \rho^+$ the solution of Riemann problem is given by a rarefaction wave defined as (see Figure 2.12)

$$\rho(x, t) = \begin{cases} \rho^- & \text{if } x < f^1(\rho^-)t \\ g\left(\frac{x}{t}\right) & \text{if } f^1(\rho^-)t \leq x < f^1(\rho^+)t \\ \rho^+ & \text{if } x > f^1(\rho^+)t \end{cases}$$

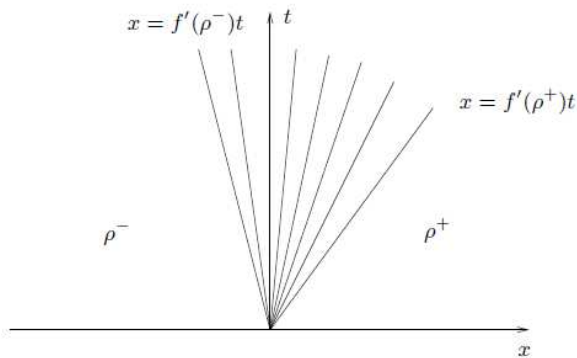


Figure 2.12 The solution to the Riemann problem when $\rho^- > \rho^+$

2.3.3 Shock and rarefactions development in traffic models

Subsequent phase to the green traffic light. Assume that cars are stopped behind a red traffic light, located at $x = 0$. Because the cars are very close to each other, we have that behind the traffic light $\rho = \rho_{\max}$ for $x < 0$. If the traffic light stops traffic for a long enough time, we can assume that there is no traffic in front of the traffic light and then $\rho = 0$ for $x > 0$.

Assume that, in $t = 0$, traffic light changes from red to green. What is the density of cars in all subsequent instants? The partial differential equation describing the conservation of the cars must be solved with the initial condition (see Figure 2.13)

$$\rho(x, 0) = \begin{cases} \rho_{\max} & \text{if } x < 0 \\ 0 & \text{if } x > 0 \end{cases}$$

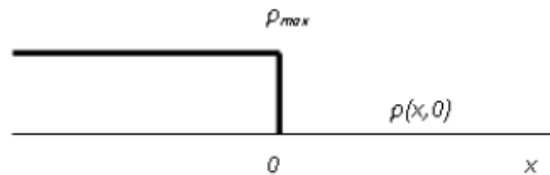


Figure 2.13 Traffic density due extremely long phase

Because $\rho^- = \rho_{\max} > 0 = \rho^+$, Riemman problem has a rarefaction wave as unique solution (see Figure 2.14).

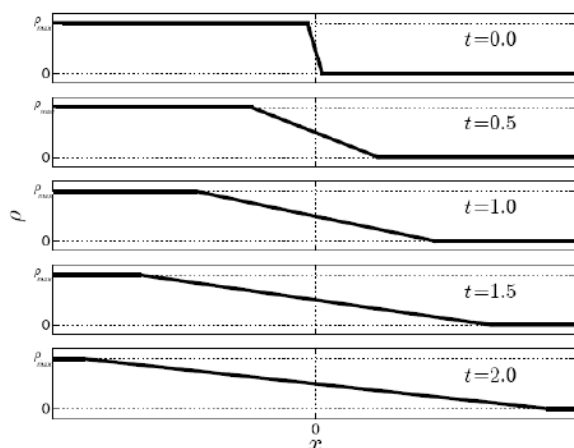


Figure 2.14 Rarefaction wave

Uniform traffic stopped by a red traffic light. We investigate what happens to a uniform traffic flux with density $\rho = \rho_0$ as result of a red traffic light located in $x = 0$. We analyze only traffic behind at the traffic lights, ignoring what happens in front of it. The red traffic light is modeled mathematically as follows. In $x = 0$, the traffic is stopped (see Figure 2.15), that is we have $v = 0$ and $\rho = \rho_{\max}$ for $t > 0$.

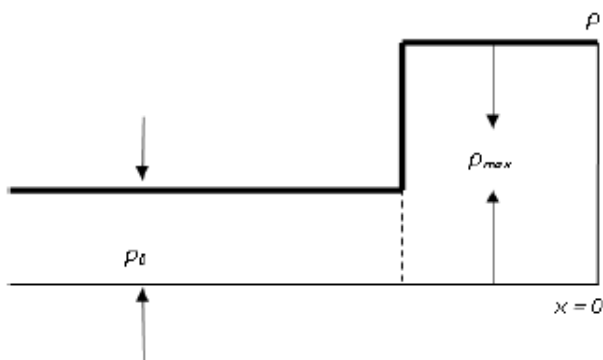


Figure 2.15 Density as result of stopped vehicular traffic

Because $\rho^- = \rho_0 < \rho_{\max} = \rho^+$, Riemann problem has a shock

wave as a unique solution.

2.3.4 Lighthill-Whitham-Richards Model with Viscosity

There are some critiques to the scalar model that are based on the fact that equation

$$\rho_t + f(\rho)_x = 0$$

generates discontinuities in finite time. In order to eliminate discontinuities in the solution it is possible to consider the equation with a viscosity term, i.e.

$$\rho_t + [f(\rho) - \mu\rho_x]_x = 0,$$

or equivalently

$$\rho_t + f'(\rho)\rho_x = \mu\rho_{xx}, \quad (1.12)$$

where μ is a positive constant.

It is possible to show that this equation is not realistic for describing the evolution of the traffic. Consider the following initial-boundary problem: the initial condition is given by

$$\rho_0(x) = \begin{cases} 1 & \text{if } -1 \leq x \leq 0 \\ 0 & \text{otherwise} \end{cases}$$

while the boundary condition $\rho(t, 0) = 1$ holds for every $t \geq 0$ (see Figure 2.16) [14].

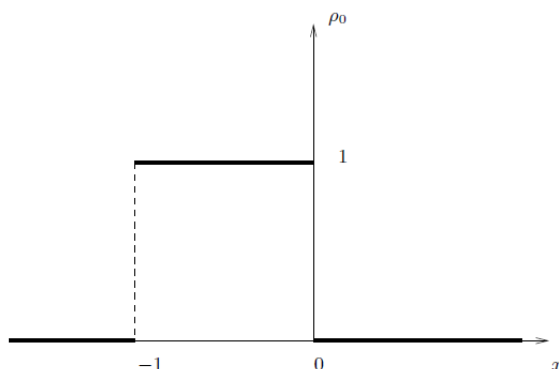


Figure 2.16 The initial configuration ρ_0

The natural traffic evolution for this problem should be $\rho(t, x) = \rho_0(x)$ for every $t \geq 0$. This is indeed a solution to the inviscid Lighthill-Whitham-Richards model with the boundary condition $\rho(t, 0) = 1$ for every $t \geq 0$. Instead, each stationary solution to (1.12) satisfies

$$f'(\rho)\rho_x = \mu\rho_{xx}.$$

Thus, the function $\rho_0(x)$ is not a stationary solution to (1.12). In detail, consider a solution $\rho'(x)$ to (1.4) with boundary condition

$$\rho'(0) = 1, \quad \lim_{x \rightarrow +\infty} \rho'(x) = 0$$

and

$$\int_{-\infty}^0 \rho'(x) dx = 1.$$

The previous condition implies that the number of cars before $x = 0$ are the same as at time $t = 0$.

Since $\rho'(x)$ is smooth, it is possible to deduce that $\rho'(x) < 1$ for $x \in [-1, 0[$. Finally, the solution to (1.12) tends to $\rho'(x)$ as $t \rightarrow +\infty$ and so some cars move backward, which is completely unrealistic.

2.4 Payne-Witham Model

Payne-Witham Model or PW model was proposed in the 1970 by [23] and [28]. It uses two Partial Differential Equations (PDE) to represent traffic dynamics.

Its general form is

$$\begin{aligned}\rho_t + (\rho v)_x &= 0 \\ v_t + vv_x &= \frac{V(\rho)-v}{\tau} - \frac{(A(\rho))_x}{\rho} + \mu \frac{v_{xx}}{\rho}.\end{aligned}\quad (1.13)$$

Table 2.1 [24] shows the different terms in this model. The first PDE is the conservation of traffic "mass" and the second one tries to emulate the fluid momentum equation.

Term	Meaning
$V(\rho)$	Equilibrium Speed
τ	Relaxation Time
$V(\rho - v)/\tau$	Relaxation
$(A(\rho))_x/\rho$	Anticipation
$\mu\rho_{xx}/\rho$	Viscosity

Table 2.1 Payne-Whitham Model Terms

The anticipation term is similar to the pressure term in fluids. In some specific models, the term is given as

$$A(\rho) = c_0^2\rho, \quad (1.14)$$

for some constant c_0 . The relaxation term is there so that in equilibrium the speed follows the value $V(\rho)$. If the viscosity is ignored and Equation (1.14) is used, then the PW model is similar to isothermal flux as

$$\begin{aligned}\rho_t + (\rho v)_x &= 0 \\ v_t + vv_x &= \frac{V(\rho)-v}{\tau} - \frac{(c_0^2\rho)_x}{\rho}.\end{aligned}$$

Equation (1.13) can be written in a conservation form by using the conservation of mass in the second equation to obtain

$$\begin{aligned}\rho_t + (\rho v)_x &= 0 \\ (\rho v)_t + (\rho v^2 + c_0^2 \rho)_x &= \rho \frac{V(\rho) - v}{\tau} + \mu v_{xx}.\end{aligned}$$

In the vector form the model becomes

$$u_t + f(u)_x = S,$$

where

$$u = \begin{pmatrix} \rho \\ \rho v \end{pmatrix}, \quad f(u) = \begin{pmatrix} \rho v \\ v^2 + c_0^2 \rho \end{pmatrix}$$

and

$$S = \begin{pmatrix} 0 \\ \rho \frac{V(\rho) - v}{\tau} + \mu v_{xx} \end{pmatrix}. \quad (1.15)$$

It is possible to write Equation (1.15) in a quasi-linear form as

$$u_t + A(u)u_x = S,$$

where

$$A(u) = \frac{\partial f}{\partial u} = \begin{pmatrix} 0 & 1 \\ c_0^2 - v^2 & 2v \end{pmatrix}.$$

The two eigenvalues of this matrix are

$$\lambda_1 = v + c_0 \text{ and } \lambda_2 = v - c_0$$

The corresponding eigenvectors are

$$v_1 = \begin{pmatrix} 1 \\ v + c_0 \end{pmatrix} \text{ and } v_2 = \begin{pmatrix} 1 \\ v - c_0 \end{pmatrix}.$$

There has been some criticism of PW model, since it mimics the fluid behavior too closely especially the fact that it shows isotropic behavior, whereas the traffic behavior should be anisotropic. Isotropic models like the fluid ones show that disturbances can travel in all directions the same way. However, for vehicular traffic that is moving forward the driver behavior should be affected by what happens in the front and not in the back. This deficiency has been overcome by other models, such as the AR and Zhang models.

2.5 Aw-Rascle Model

This model is designed to model the anisotropic traffic behavior and it is based on the system:

$$\begin{aligned}\rho_t + (\rho v)_x &= 0 \\ [v + p(\rho)]_t + v [(v + p(\rho))]_x &= \frac{V(\rho) - v}{\tau},\end{aligned}\quad (1.16)$$

where $V(\rho)$ is the equilibrium speed and $p(\rho)$ is the "pressure", an increasing function of the density defined as

$$p(\rho) = c_0^2 \rho^\gamma,$$

where $\gamma > 0$ and $c_0 = 1$.

For further analysis, the relaxation term is ignored. For smooth solutions system the Equation (1.16) is equivalent to the following system obtained by multiplying the first equation by $p'(\rho)$ in (1.16) and then adding that to the second equation. These operations lead to to the model defined in the following form:

$$\begin{aligned}\rho_t + (\rho v)_x &= 0 \\ v_t + [v - \rho p'(\rho)] v_x &= 0.\end{aligned}$$

The AR model in conservation form is given by:

$$\begin{aligned}\rho_t + (\rho v)_x &= 0 \\ [\rho(v + p(\rho))]_t + [\rho v(v + p(\rho))]_x &= 0.\end{aligned}$$

Now, a new variable $m = \rho(v + p(\rho))$ is defined, so that the model can be written as

$$\begin{aligned}\rho_t + (m - \rho p)_x &= 0 \\ m_t + \left(\frac{m^2}{\rho} - mp\right)_x &= 0.\end{aligned}$$

In the vector form this model becomes

$$u_t + f(u)_x = 0,$$

where

$$u = \begin{pmatrix} \rho \\ m \end{pmatrix}, \text{ and } f(u) = \begin{pmatrix} m - \rho(p) \\ \frac{m^2}{\rho} - mp \end{pmatrix}.$$

It is possible to write this vector form equation in the quasi-linear form and obtain the eigenvalues and eigenvectors for the system.

The quasi-linear form is

$$u_t + A(u)u_x = 0,$$

where

$$A(u) = \frac{\partial f}{\partial u} = \begin{pmatrix} -(\gamma + 1)p & 1 \\ -\frac{m^2}{\rho^2} - \frac{\gamma pm}{\rho} & \frac{2m}{\rho} - p \end{pmatrix}.$$

The two eigenvalues of the matrix are

$$\lambda_1 = v \text{ and } \lambda_2 = v - \gamma p.$$

The corresponding eigenvectors are

$$v_1 = \begin{pmatrix} 1 \\ v + (\gamma + 1)p \end{pmatrix} \text{ and } v_2 = \begin{pmatrix} 1 \\ v + p \end{pmatrix}.$$

2.6 Zhang Model

This model retains the anisotropic traffic property, because its momentum equation is derived from a microscopic car following model.

The Zhang model is based on the following set of PDEs:

$$\rho_t + (\rho v)_x = 0$$

$$v_t + [v + \rho V'(\rho)]v_x = \frac{V(\rho)-v}{\tau}.$$

Ignoring the relaxation term, the conservation form of this model becomes

$$\rho_t + (\rho v)_x = 0$$

$$[\rho(v - V(\rho))]_t + [\rho v(v - V(\rho))]_x = 0.$$

A new variable $m = \rho(v - V(\rho))$ is defined, so the model can be written as

$$\rho_t + (m - \rho P)_x = 0$$

$$m_t + \left[\frac{m^2}{\rho} - mP \right]_x = 0.$$

In the vector form, this model is

$$u_t + f(u)_x = 0,$$

where $u = \begin{pmatrix} \rho \\ m \end{pmatrix}$ and $f(u) = \begin{pmatrix} m + \rho V(\rho) \\ \frac{m^2}{\rho} + mV(\rho) \end{pmatrix}$.

It is possible to write this vector form in the quasi-linear form and obtain the eigenvalues and the eigenvectors for the system. The quasi-linear form is

$$u_t + A(u)u_x = 0,$$

where

$$A(u) = \frac{\partial f}{\partial u} = \begin{pmatrix} \rho V'(\rho) + V(\rho) & 1 \\ -\frac{m^2}{\rho^2} + mV'(\rho) & \frac{2m}{\rho} + V(\rho) \end{pmatrix}.$$

The two eigenvalues of this matrix are

$$\lambda_1 = v \text{ and } \lambda_2 = v + \rho V'(\rho).$$

The corresponding eigenvectors are

$$v_1 = \begin{pmatrix} 1 \\ v - V(\rho) - \rho V'(\rho) \end{pmatrix} \text{ and } v_2 = \begin{pmatrix} 1 \\ v - V(\rho) \end{pmatrix}.$$

2.7 Third order Models

The first third order model was proposed in 1995 by Dirk Helbing. The main idea was to consider non only equations for density and velocity, but also for the variance θ that becomes important for describing and predicting traffic jams on roads. In fact, fast increment of the variance implies queue formation in car traffic.

The exact model proposed by Helbing is the following:

$$\begin{aligned}\rho(t, x) &= \rho_t + (\rho v)_x = 0 \\ v_t + vv_x + \frac{1}{\rho}(\rho\theta)_x &= \frac{1}{\tau}(v_e(\rho) - v) + \frac{\mu}{\rho}v_{xx} \\ \theta_t + v\theta_x + 2\theta v_x &= 2\frac{\mu}{\rho}(v_x)^2 + \frac{k}{\rho}\theta_{xx} + \frac{2}{\tau}(\theta_e(\rho) - \theta),\end{aligned}$$

where θ_e and v_e are given smooth functions of the density ρ , while μ , k , τ are positive constants. The coefficient k is called *kinetic coefficient*. The quantity

$$J(t, x) := -k\theta_x$$

describes a flux of speed variance leading to a spatial smoothing of θ . The term originates from the finite reaction and bracking time, which causes a delayed adaption of speed to traffic situation. The term

$$\frac{2}{\tau}(\theta_e(\rho) - \theta)$$

results from the drivers' attempt to drive with their desired speeds and from drivers' interactions, i.e. from deceleration in a situation when a fast car can not overtake a slower one.

2.8 Multilane Model

Multiplane model is an extension of LWR model. The main novelty is considering an unidirectional one-dimensional road with n lanes.

The macroscopic variables considered here are the density ρ of cars and the average speed v across all the lanes. Thus we have

$$\rho = \sum_{i=1}^n \rho_i$$

and

$$\rho v = \sum_{i=1}^n \rho_i v_i,$$

where ρ_i and v_i are respectively the density and the average speed of cars in the i -th lane.

In a multilane road, it is possible to observe different traffic behaviour based on the density of traffic. When traffic is low, changing lane and overcome cars is easy and so the equilibrium speed for cars is high. When traffic is high, these actions become complicate and difficult, so that the equilibrium speed for cars is low. The typical situation involves two different equilibria for the average speed of cars. This is described by two functions $w_1(\rho)$ and $w_2(\rho)$ defined on interval $[0, \rho_{\max}]$ such that

$$w_1(\rho) > w_2(\rho),$$

for every $\rho \in [0, \rho_{\max}[$ and $w_1(\rho_{\max}) = w_2(\rho_{\max}) = 0$. When the density ρ is less than a critical value ρ_1^- , then the average speed is described by the function w_1 , while when the density ρ is greater than a value ρ_2^- , then the average speed is described by the function w_2 (see Figure 2.17) [14].

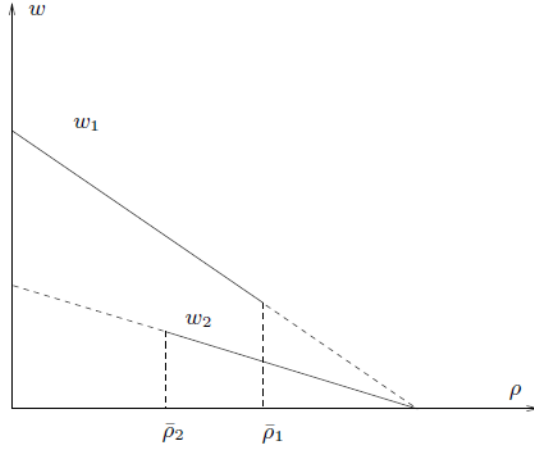


Figure 2.17 The functions w_1 and w_2 for the multilane model

Defining $\alpha = v - w_1(\rho)$, the system is given by:

$$\begin{aligned} \rho_t + (\rho v)_x &= 0 \\ \alpha_t + v\alpha_x &= \begin{cases} -\frac{\alpha}{\epsilon} & \rho < R(v) \\ \frac{(w_2(\rho) - w_1(\rho)) - \alpha}{\epsilon} & \rho \geq R(v) \end{cases} \end{aligned} \quad (1.17)$$

where $R(v)$ is a monotone non-decreasing function defined in \mathbb{R}^+ satisfying

$$R(v) = \rho_2^-, \quad \forall 0 \leq v \leq w_2(\rho_2^-)$$

and

$$R(v) = \rho_1^-, \quad \forall v \geq w_1(\rho_1^-),$$

and ϵ is a small positive constant.

Notice that (1.17) in terms of ρ and v becomes

$$\begin{aligned} \rho_t + (\rho v)_x &= 0 \\ v_t + (v + \rho w_1'(\rho))v_x &= \begin{cases} -\frac{w_1(\rho) - v}{\epsilon} & \rho < R(v) \\ \frac{(w_2(\rho) - v)}{\epsilon} & \rho \geq R(v) \end{cases} \end{aligned}$$

Chapter 3

Fluid-dynamic model for vehicular traffic networks

3.1 Assumptions

A road network is composed of a finite numbers of roads (**arcs**) I_k , $k = 1, \dots, N$ that are modeled by intervals $[a_k, b_k]$ (with one of the two ends possibly finite) joining up at intersections J (**vertex**).

For each intersection two sets, both non-empty, differ:

- $Inc(J)$ set of incoming roads in intersection J .
- $Out(J)$ set of outgoing roads from intersection J .

It is possible to represent a road network as an directed graph (see Figure 3.1) where directed arc $I_k = [a_k, b_k]$ is k-th road crossed in the direction that goes from a_k to b_k ; a node J represents an intersection for which incoming roads are given by $Inc(J)$ and outgoing roads are given by $Out(J)$.

For roads that do not join up at intersections (and that are not infinite) assignment of boundary conditions is assumed and corresponding boundary problem is solved (green and red nodes in Figure 3.1).

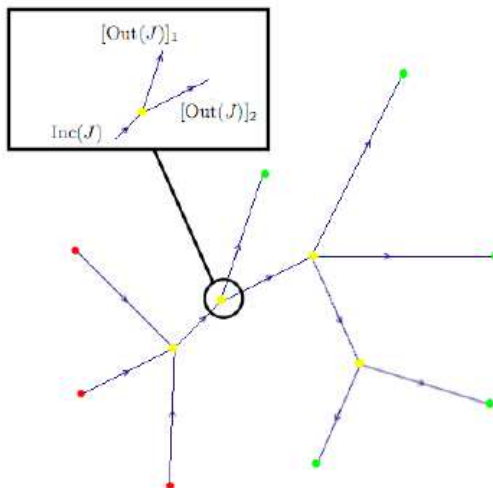


Figure 3.1 Example of simple road network

It is assumed that, for each arc I_k , initial distribution $\rho_{k,0}$ of density ρ_k is known. Furthermore, it is assumed that the evolution of the traffic on each road is described by a conservation law for cars (LWR model):

$$\rho_t + f(\rho)_x = 0,$$

where $\rho : (x, t) \in R_+ \times R \rightarrow \rho(x, t) \in [0, \rho_{\max}]$ is the car density, $f(\rho) = v\rho$ is the flux and $v = v(x, t)$ is the velocity.

It is assumed that the flux $f \in C^2([0, \rho_{\max}])$ is a strictly concave function, $f(0) = f(\rho_{\max}) = 0$ and has a single maximum point within $\sigma \in]0, \rho_{\max}[$.

In order to simplify the notation, we will suppose $\rho_{\max} = 1$.

Key role is played by intersections where the system is under-determined, while using Rankine-Hugoniot condition that for an intersection $n \times m$ (n incoming roads and m outgoing roads) is

$$\sum_{i=1}^n f(\rho_i(t, b_i)) = \sum_{j=n+1}^{n+m} f(\rho_j(t, b_j)),$$

where ρ_i , $i = 1, \dots, n$, are densities on incoming roads, while ρ_j , $j = n + 1, \dots, n + m$ are car densities on outgoing roads from intersection.

Basic ingredient for solving Cauchy problems at intersections (**vertices**) through *wave-front-tracking* method is represented by the solution of **Riemann problems**, special Cauchy problem with constant initial conditions on each incoming and outgoing road. The discontinuity in this case is represented by the vertex itself.

In order to describe the dynamics at vertices, we introduce the following definitions:

Definition 2.1 *A Riemann Solver (RS) for the vertex J is a map $RS : [0, \rho_{\max}]^n \times [0, \rho_{\max}]^m \rightarrow [0, \rho_{\max}]^n \times [0, \rho_{\max}]^m$ that associates with Riemann data $\rho_0 = (\rho_{1,0}, \dots, \rho_{n+m,0})$ at J a vector $\bar{\rho} = (\bar{\rho}_1, \dots, \bar{\rho}_{n+m})$, so that the solution on an incoming road I_i , $i = 1, \dots, n$ is given by the waves produced by the Riemann problem $(\rho_{i,0}, \bar{\rho}_i)$, and on an outgoing road I_j , $j = n + 1, \dots, n + m$ by the waves produced by the Riemann problem $(\bar{\rho}_j, \rho_{j,0})$. We require the consistency condition*

$$(CC) \quad RS(RS(\rho)) = RS(\rho_0)$$

A RS is further required to guarantee the fulfillment of the following properties:

(H1) The waves generated from the vertex must have negative velocities on incoming arcs and positive velocities on outgoing ones. This is a *consistency condition* to well describe the dynamics at vertex.

(H2) Relation (2.1) holds for solutions to Riemann problems at the vertex. This is necessary to have a *weak solution* at the vertex.

(H3) The map $\rho_0 \rightarrow f(\bar{\rho})$ is continuous. This is a *regularity condition*, necessary to have a well-posed theory.

In order to ensure that Riemann problems have unique solution at intersections, we assume the following rules by considering two RS at vertices:

- **(R1)** We assume that:

(A) the traffic of incoming roads is distributed on outgoing roads according to fixed coefficients;

(B) fulfilling (A), drivers move in order to maximize the incoming flux.

- (R2) We assume that the flux through a vertex (intersection) is maximized both over incoming and outgoing arcs (roads).

Given a $n \times m$ intersection, in order to formalize assumption (A) a traffic distribution matrix is fixed:

$$A = \{\alpha_{ji}\}_{j=n+1, \dots, n+m; i=1, \dots, n} \in \mathbb{R}^{m \times n}$$

such that

$$0 < \alpha_{ji} < 1, \quad \sum_{j=n+1}^{n+m} \alpha_{ji} = 1$$

For each $i = 1, \dots, n$ and $j = n + 1, \dots, n + m$ elements of A , α_{ji} , state probability that drivers coming from the i -th incoming road decide to take the j -th outgoing road. We observe that only rule (A) does not guarantee the uniqueness but, combined with rule (B) makes solution of Riemann problems unique.

Notice that if $m < n$ (that is the number of incoming roads is greater than outgoing ones) it is necessary to introduce an additional rule.

For example, if $m = 1$ and $n = 2$ it is possible to define (and fix) a **priority parameter** $q \in [0, 1]$ and assign the following rule:

(C) not all cars can go in the outgoing road. Let C be the amount of cars that can go in, then qC is the percentage of cars from the first incoming road and $(1 - q)C$ is the percentage of cars from the second incoming road.

Hereafter, we will denote with the term “**RS Base**” (or simply “**Base**”) the Riemann Solver (R1) satisfying rules (A), (B) and (C).

Now, we describe how to determine the solution of Riemann problem.

Two sets are defined:

$$\Omega_i = [0, f(\bar{\rho}_{i,0})], \quad i = 1, \dots, n$$

$$\Omega_j = [0, f(\bar{\rho}_{j,0})], \quad j = n + 1, \dots, n + m$$

where

$$\bar{\rho}_{i,0} = \begin{cases} \rho_{i,0} & \text{if } 0 \leq \rho_{i,0} \leq \sigma \\ \sigma & \text{if } \sigma \leq \rho_{i,0} \leq 1 \end{cases} \quad i = 1, \dots, n$$

$$\bar{\rho}_{j,0} = \begin{cases} \sigma & \text{if } 0 \leq \rho_{i,0} \leq \sigma \\ \rho_{j,0} & \text{if } \sigma \leq \rho_{i,0} \leq 1 \end{cases} \quad j = n + 1, \dots, n + m.$$

Maximum incoming and outgoing fluxes are given by:

$$\Omega = \{(\gamma_1, \dots, \gamma_n) \in \Omega_1 \times \dots \times \Omega_n \mid A \cdot (\gamma_1, \dots, \gamma_n)^t \in \Omega_{n+1} \times \dots \times \Omega_{n+m}\}.$$

Notice that Ω is a convex set determined by linear constraints.

Moreover, Rule (A) implies (H2). Thus, Rule (B) is equivalent to maximize only over incoming fluxes, then outgoing ones can be determined by Rule (A).

Finally, Rule (A) and Rule (B) correspond to a Linear Programming Problem: maximize the sum of fluxes from incoming roads over the region Ω .

Such problem admits always a solution, which is unique provided the cost function gradient (here the vector with all components equal to 1) is not orthogonal to the linear constraints describing the set Ω .

Obtained the incoming fluxes that are solution of Riemann problem $\bar{\gamma}_i$, $i \in \{1, \dots, n\}$, in order to satisfy the rule (B), $\bar{\rho}_i$ is chosen such that

$$\hat{\rho}_i \in \begin{cases} \{\rho_{i,0}\} \cup [\tau(\rho_{i,0}), 1] & \text{if } 0 \leq \rho_{i,0} \leq \sigma \\ [\sigma, 1] & \text{if } \sigma \leq \rho_{i,0} \leq 1 \end{cases} \quad i = 1, \dots, n, \quad (2.1)$$

where $\tau : [0, 1] \rightarrow [0, 1]$ is an application such that:

1. $f(\tau(\rho)) = f(\rho)$ for each $\rho \in [0, 1]$;

2. $\tau(\rho) \neq \rho$ for each $\rho \in [0, 1] \setminus \{\sigma\}$.

Clearly, τ is well defined and satisfies the following conditions:

$$\begin{aligned} 0 \leq \rho \leq \sigma &\iff \sigma \leq \tau(\rho) \leq 1 \\ \sigma \leq \rho \leq 1 &\iff 0 \leq \tau(\rho) \leq \sigma \end{aligned}$$

By recalling rule (A) we have:

$$\bar{\gamma}_i = \sum_{j=1}^n \alpha_{ji} \bar{\gamma}_j, \quad j = n+1, \dots, n+m \quad (2.2)$$

and

$$\bar{\rho}_j \in [0, 1]$$

such that

$$\begin{aligned} f(\bar{\rho}_j) &= \bar{\gamma}_j \\ \bar{\rho}_j &\in \begin{cases} [0, \sigma] & \text{if } 0 \leq \rho_{j,0} \leq \sigma \\ \{\rho_{j,0}\} \cup [0, \tau(\rho_{j,0})[& \text{if } \sigma \leq \rho_{j,0} \leq 1 \end{cases} \quad j=n+1, \dots, n+m. \end{aligned} \quad (2.3)$$

The solution on each road is given by solution of Riemann problem with data $(\rho_{i,0}, \bar{\rho}_i)$ for incoming roads and $(\bar{\rho}_j, \rho_{j,0})$ for outgoing roads.

3.2 Solution of Riemann problem for specific cases

Case 1: 2×1 Intersection

We define a Riemann Solver at intersection satisfying rules (A) and (B). In particular, we consider a 2×1 Intersection (two incoming roads and one outgoing road). In this case, since $m = 1 < 2 = n$ we need the additional rule (C).

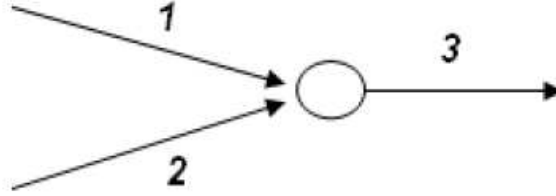


Figure 3.2 Example of 2×1 Intersection

We analyze the intersection shown in Figure 3.2: in detail, 1 and 2 are incoming roads and 3 is the only outgoing road. The solution of Riemann problem with initial datum $(\rho_{1,0}, \rho_{2,0}, \rho_{3,0})$ is created as follows. Because we want maximize the traffic flux through the intersection (rule B) we set:

$$\bar{\gamma}_3 = \min \{ \gamma_1^{\max} + \gamma_2^{\max}, \gamma_3^{\max} \},$$

where $\gamma_i^{\max}, i = 1, 2$ is maximum flux on incoming roads and γ_3^{\max} is the maximum flux on outgoing road [10].

$$\gamma_i^{\max} = \begin{cases} f(\rho_{i,0}) & \text{if } \rho_{i,0} \in [0, \rho_{\max}] \\ f(\sigma) & \text{if } \rho_{i,0} \in [\rho_{\max}, 1] \end{cases} \quad i = 1, 2$$

$$\gamma_3^{\max} = \begin{cases} f(\sigma) & \text{if } \rho_{3,0} \in [0, \rho_{\max}] \\ f(\rho_{3,0}) & \text{if } \rho_{3,0} \in [\rho_{\max}, 1] \end{cases}$$

Notice that matrix A defined by rule (A) is only column vector $(1,1)$, so any additional restriction is not given. This is due to the fact that there is only a outgoing road and so cars must necessarily flux towards this road.

Consider now on plane (γ_1, λ_2) the line

$$\gamma_2 = \frac{1-q}{q} \gamma_1$$

defined according to rule (C). Let P intersection point of such line with line $\gamma_1 + \gamma_2 = \bar{\gamma}_3$.

Final fluxes must belong to region:

$$\Omega = \{(\gamma_1, \gamma_2) : 0 \leq \gamma_i \leq \gamma_i^{\max}, \quad 0 \leq \gamma_1 + \gamma_2 \leq \bar{\gamma}_3, \quad i = 1, 2\}.$$

We must distinguish two different cases (see Figure 3.3):

- P belongs to Ω
- P is outside Ω

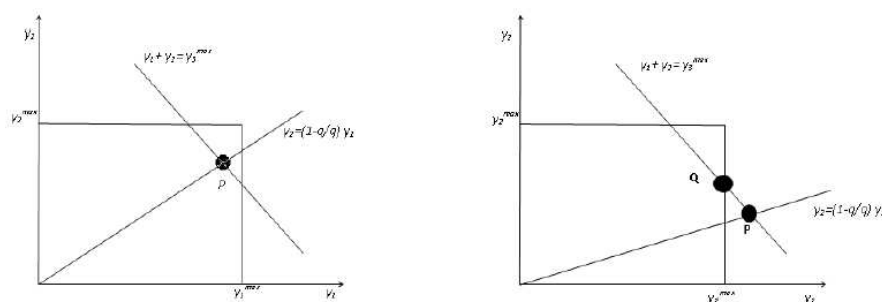


Figure 3.3 2×1 Intersection: Case 1 and 2

In the first case, we let $(\bar{\gamma}_1, \bar{\gamma}_2) = P$ while, in the second case we let $(\bar{\gamma}_1, \bar{\gamma}_2) = Q$ where Q is projection of P on $\Omega \cap \{(\gamma_1, \gamma_2) : \gamma_1 + \gamma_2 = \bar{\gamma}_3\}$. Once $\bar{\gamma}_1$ and $\bar{\gamma}_2$ have been determined (and consequently $\bar{\gamma}_3$ by (2.2)) it is possible to univocally calculate $\bar{\rho}_i$, $i \in \{1, 2, 3\}$ by (2.1) and (2.3).

Case 2: 2×2 Intersection

Consider case where $n = 2$ incoming roads and $m = 2$ outgoing roads (see Figure 3.4).

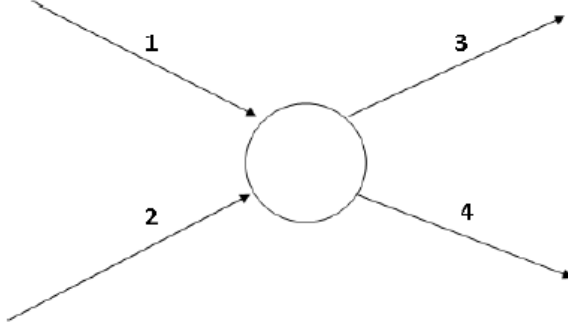


Figure 3.4 Example of 2×2 Intersection

For an intersection J we state densities on incoming roads 1 and 2 as ρ_1 and ρ_2 and on outgoing roads 3 and 4 as ρ_3 and ρ_4 , and initial conditions as $(\rho_{1,0}, \rho_{2,0}, \rho_{3,0}, \rho_{4,0})$.

We define distribution matrix as

$$A = \begin{pmatrix} \alpha & \beta \\ 1 - \alpha & 1 - \beta \end{pmatrix}.$$

Let's see how construct the solution of Riemann problem with initial data defined previously.

Because we want maximize the traffic flux specified as Γ through-out the intersection (rule B), we set

$$\Gamma = \min \{ \Gamma_{in}^{\max}, \Gamma_{out}^{\max} \},$$

where $\Gamma_{in}^{\max} = \gamma_1^{\max} + \gamma_2^{\max}$ and $\Gamma_{out}^{\max} = \gamma_3^{\max} + \gamma_4^{\max}$ and maximum flux within incoming and outgoing roads, respectively, γ_i^{\max} , $i = 1, 2$ and γ_j^{\max} , $j = 3, 4$ are calculated:

$$\gamma_i^{\max} = \begin{cases} f(\rho_{i,0}) & \text{if } \rho_{i,0} \in [0, \rho_{\max}] \\ f(\sigma) & \text{if } \rho_{i,0} \in [\rho_{\max}, 1] \end{cases} \quad i = 1, 2$$

$$\gamma_j^{\max} = \begin{cases} f(\sigma) & \text{if } \rho_{j,0} \in [0, \rho_{\max}] \\ f(\rho_{j,0}) & \text{if } \rho_{j,0} \in [\rho_{\max}, 1] \end{cases} \quad j = 3, 4.$$

Final fluxes must belong to the region:

$$\Omega = \{(\gamma_1, \gamma_2) : 0 \leq \gamma_i \leq \gamma_i^{\max}, 0 \leq \alpha\gamma_1 + \beta\gamma_2 \leq \gamma_3, \\ 0 \leq (1 - \alpha)\gamma_1 + (1 - \beta)\gamma_2 \leq \gamma_4 \quad i = 1, 2\},$$

as shown in Figure 3.5.

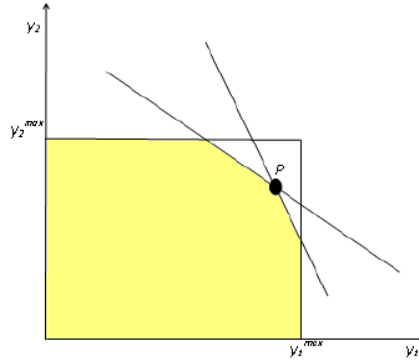


Figure 3.5 2×2 Intersection - Final fluxes region

3.3 Alternative Riemann Solver at Intersections

We describe some new models that can be defined starting from RS (R1) and RS (R2). In detail, we define some additional rules (N) for $N=1, \dots, 4$ and then identify new RS as follows:

- (i) we use rule (N) to determine the fluxes in incoming roads (arcs). Then, by rule (A) it is possible to determine the fluxes on outgoing roads. Thus, we get new RSs called (R1-N);
- (ii) we use (R2) to determine the through flux and rule (N) to determine fluxes on incoming or outgoing roads. Thus, we get new RSs called (R2-N).

In order to simplify the presentation, we restrict ourselves to the case of 2×2 intersections (vertices), i.e. intersections with two incoming and two outgoing roads (arcs).

Notation 2.1: The incoming roads are I_1 and I_2 , the outgoing ones are I_3 and I_4 . The initial datum is denoted by $\rho_0 = (\rho_{1,0}, \dots, \rho_{4,0})$ and the initial fluxes are denoted by $\gamma_0 = (\gamma_{1,0}, \dots, \gamma_{4,0})$. The vector of fluxes over incoming roads is $\gamma_{in} = (\gamma_1, \gamma_2)$ and over outgoing roads is $\gamma_{out} = (\gamma_3, \gamma_4)$. The matrix A of rule (A) is

$$\begin{pmatrix} \alpha & \beta \\ 1 - \alpha & 1 - \beta \end{pmatrix}$$

We also use the following notations:

$$\Omega_{in} = [0, \gamma_1^{\max}] \times \dots \times [0, \gamma_n^{\max}],$$

$$\Omega_{out} = [0, \gamma_{n+1}^{\max}] \times \dots \times [0, \gamma_{n+m}^{\max}],$$

$$\bar{\Omega}_{in} = \{\gamma \in \Omega_{in} : A \cdot \gamma \in \Omega_{out}\}.$$

Notice that the region $\bar{\Omega}_{in}$ is determined by the linear constraints given by the maximal fluxes on each arc. We give the following definition:

Definition 2.2: We say the incoming arc (road) I_i is an active constraint for J if $\gamma(\bar{\rho}_i) = \gamma_i^{\max}$.

Similarly for outgoing arcs (roads).

In detail, an incoming arc I_i is an active constraint if $\bar{\rho}_i \in [0, \sigma]$ and an outgoing arc I_j is an active constraint if $\bar{\rho}_j \in [\sigma, \rho_{\max}]$.

Model 1. (Equilibrium and maximization)

We fix the rule:

(Rule 1). The incoming flux is determined by:

$$\max_{\gamma_{in} \in \bar{\Omega}_{in}} v \cdot \gamma_{in},$$

where $v \in \{w \in \mathbb{R}^2 : w_i \geq 0, \quad i = 1, 2\}$ is fixed.

The physical meaning of the model is the following. The traffic through the intersection (vertex) tends to an equilibrium of

the flux ratios, while maximizing the total through flux. The proportion equilibrium is determined by the physical features of the intersection, e.g. by the fact that it represents a junction in which a road is more important than the other.

Notice that the flux vector of the true solution may be quite different from the expected equilibrium value v .

Hereafter, we will denote with the term “**RS 1**” the alternative Riemann Solver described by Model 1.

Model 2. (Equilibrium then maximization)

We fix the rule:

(**Rule 2**). The incoming flux is determined by:

$$\max_{\gamma_{in} \in V \cap \bar{\Omega}_{in}} \gamma_{in} \cdot (1, 1),$$

where $V = \{tv : t \in \mathbb{R}\}$ and $v \in \mathbb{R}^2$ is fixed.

The physical meaning of the model is the following. The flux proportions are now strictly fulfilled, then the flux is maximized among the possible choices. In some senses, here the traffic flux is more influenced by the physical structure of the intersection. For instance, this solver may correspond to a junction with a traffic light having a fixed schedule of red-green times, while the previous one represents a light with a variable schedule. Thus, the timing of the light is independent of the effective incoming traffic for this solver, while it is adjusted according to the incoming traffic at previous case.

Hereafter, we will denote with the term “**RS 2**” the alternative Riemann Solver described by Model 2.

Model 3. (Variable equilibrium then maximization)

We fix the following rule:

(**Rule 3**). The incoming flux is determined by:

$$\max_{\gamma_{in} \in V(\gamma_0) \cap \bar{\Omega}_{in}} \gamma_{in} \cdot (1, 1),$$

where $V(\gamma_0) = \{tv(\gamma_0) : t \in \mathbb{R}\}$ and $v : \mathbb{R}^2 \rightarrow \mathbb{R}^2$ is a fixed function.

The physical meaning of the model is the following. The flux proportions are strictly fulfilled, then the flux is maximized among the possible choices. However, the flux proportions depend on incoming fluxes. This is, roughly speaking, an intermediate choice between the previous two models.

Model 4. (Parametric equilibrium then maximization)

We fix the following rule:

(Rule 4). The incoming flux is determined by:

$$\max_{\gamma_{in} \in V(\gamma_0, \Theta) \cap \bar{\Omega}_{in}} \gamma_{in} \cdot (1, 1),$$

where $V(\gamma_0, \Theta) = \{tv(\gamma_0, \Theta) : t \in \mathbb{R}\}$, $\Theta \in \mathbb{R}^p$ represents some time evolving parameters and $v : \mathbb{R}^2 \times \mathbb{R}^p \rightarrow \mathbb{R}^2$ is a fixed function.

The physical meaning of the model is the following. The flux proportions are strictly fulfilled, then the flux is maximized among the possible choices. However, the flux proportions depend on additional parameters Θ .

The parameters Θ may have different meanings:

- aggressivity parameters describing the attitude of the traffic from some roads with respect to others;
- source-destination parameters describing the traffic type as reported in [15];
- traffic population parameters distinguishing among vehicles of different types as cars, trucks, buses, etc. as reported in [4].

The parameters Θ may vary both inside the roads and time. A possible evolution equation is derived by the following semi-linear equation:

$$\Theta_t + w(\Theta, \rho)\Theta_x = 0,$$

where w is the velocity depending on the density ρ . For example, consider source-destination parameters. It is obvious to

assume that the average velocity does not depend on such parameters (i.e. it is independent of the source or the destination of vehicles). For this reason, one can set $w(\Theta, \rho) = v(\rho)$ [15] [19].

About multi-populations, it is obvious to assume that w depends on the traffic type. In fact, one expects the average velocity depends on the type of vehicle.

In the following subsections, we analyze the properties of the vertex-dynamics corresponding to the additional rules just defined.

3.3.1 The Riemann Solver (R1-1)

It is necessary to impose some conditions in order to determine a unique solution. In detail, we have the following:

Proposition 2.1: Assume that v is parallel either to the vector (α, β) or to the vector $((1 - \alpha), (1 - \beta))$, then Rule (A) and Rule (1) do not determine a unique solution for some initial data.

Proof: The region $\bar{\Omega}_{in}$ is determined also by the linear constraints:

$$\alpha\gamma_1 + \beta\gamma_2 \leq \gamma_3^{\max}, \quad (1 - \alpha)\gamma_1 + (1 - \beta)\gamma_2 \leq \gamma_4^{\max}.$$

If the assumptions hold, the the vector v is orthogonal to one of these constraints. So, it is clear that a unique solution may not exist.

In order to overcome this problem, one possibility is to use Rule (C) by considering v as priority vector. In detail, we define the following rule:

(C') we assume Rule (C) taking v as *priority vector*.

Proposition 2.2: We have the following:

- (i) Rules (A), (1) and (C') determine a unique solution for every initial datum.
- (ii) For the solution in (i), (CC) of Definition 2.1 holds true.
- (iii) For the solution in (i), (H3) holds true.

Proof: The first statement is verified by construction.

For (ii), observe that if I_i is an active constraint the the solution does not produce any wave on I_i . If we apply the R1-1 to $\bar{\rho}$. Then the maximization of Rule (1) is done on a region enlarged only by non-active constraints. for this reason. the solution is the same for ρ . In other words, (CC) holds true.

Finally, for (iii) it is enough to notice that the linear constraints over the incoming fluxes depend all in a continuous fashion on γ_0 , thus on the initial datum. The latter determines both the region $\bar{\Omega}_{in}$ and the maximal value solution of Rule (1).

3.3.2 The Riemann Solver (R1-2)

Rule (2) is the most efficient for determining solutions to Riemann Problems, as shown below.

Proposition 2.3: We have the following:

- (i) Rules (A) and (2) determine a unique solution for every initial datum.
- (ii) For the solution in (i), (CC) of Definition 2.1 holds true.
- (iii) For the solution in (i), (H3) holds true.

Proof: In order to prove (i), notice that the set $S = V \cap \bar{\Omega}_{in}$ is convex because intersection of convex sets. S is one dimensional (segment) and non-empty because the origin belongs to both sets. Finally, the set S is contained in the positive orthant $P = \{\gamma \in \mathbb{R}^2 : \gamma_i > 0\}$. Therefore, S is not orthogonal to the vector $(1, 1)$.

The proofs of (ii) and (iii) are as for Proposition 2.3.

3.3.3 The Riemann Solver (R1-3)

Set $P = \{\gamma \in \mathbb{R}^2 : \gamma_i > 0\}$. In order for the solution to have a reasonable meaning, the map v should take values inside P , thus it is possible to compone the map with the projection π of $\mathbb{R}^2 \setminus \{0\}$ on to S^1 , given by $\pi(x) = x / |x|$.

In addition, if the vector γ_0 does not belong to P (e.g. initial data with a zero flux form one or both incoming arc), then the map v is not relevant to determine the solution, thus it is possible to assume it is defined on P . Finally, to simplify the treatment the following assumption is made.

(V) The map v is defined on P , takes values in $P \cap S^1$ and is smooth.

Under assumption (V), it is possible to define the following set:

$$X(v) = \{\gamma \in P \cap S^1 : v(\gamma) = \gamma\}.$$

$X(v)$ is the set of equilibrium for the map RS composed with π , i.e. the set of points γ such that $\pi(RS(\gamma)) = \gamma$. Then, we have the following:

Proposition 2.4: Consider Rules (A) and (3) with $v(\cdot)$ satisfying (V), and the corresponding RS R1-3. Then, R1-3 satisfies the compatibility condition (CC) of Definition 2.1 iff $v(\gamma) \in X(v)$ for every $\gamma \in P$.

Proof: Consider a vector $\gamma \in P$ such that $v(\gamma) \notin X(v)$ and assume $\alpha + \beta > 1$ (the other case being similar). Then, consider an initial datum ρ_0 such that $(\gamma_{1,0}, \gamma_{2,0}) = \gamma$, $\gamma_3^{\max} = \alpha v(\gamma)_1 + \beta v(\gamma)_2$, where $v(\gamma)_i$ are the components of $v(\gamma)$ and finally $\gamma_4^{\max} = f(\sigma)$. Then the vector of solutions fluxes over incoming arcs, namely $(f(\bar{\rho}_1), f(\bar{\rho}_2))$ is parallel to $v(\gamma)$. Now, $R1 - 3(\bar{\rho})$ determines an incoming flux on the line $\{tv(v(\gamma))t \geq 0\}$. But $v(v(\gamma)) \neq v(\gamma)$ because $v(\gamma) \notin X(v)$, then necessarily $R1 - 3(\bar{\rho}) = R1 - 3(R1 - 3(\rho_0)) \neq R1 - 3(\rho_0)$.

In this way, in order to have the consistency property (CC) by Proposition 2.4 the map v must take values inside $X(v)$. It is possible to put further restrictions on v for the sake of uniqueness:

Proposition 2.5: Consider Rules (A), (3) with $v(\cdot)$ satisfying (V), and the corresponding RS R1-3. Then, R1-3 gives rise to unique weak solutions to Riemann Problems at J iff $X(v)$ is a singleton. In this case R1-3 coincides with R1-2.

Proof: Assume by contradiction that $X(v)$ is not a singleton.

Define $\bar{\Omega} = \{\gamma : (A\gamma)_i \leq f(\sigma), i = 1, 2\}$, i.e. the set of incoming fluxes with respect to the constraints on free outgoing arcs. Take

$v_1 \neq v_2$ with $v_k \in X(v)$, $k = 1, 2$ and let $\bar{v}_k = t_k v_k$, where $t_k = \max \{t : tv_k \in \bar{\Omega}\}$. Consider a Riemann Problem at J with initial datum ρ_0^k such that $(\gamma_{1,0}^k, \gamma_{2,0}^k)$ is parallel to v_k and $\rho_{i,0}^k, \rho_{j,0}^k$ are good data. Then, $(\bar{\gamma}_1^k, \bar{\gamma}_2^k) = \bar{v}_k$.

The Riemann Problem with initial datum ρ_0^1 admits the solution given by R1-3(ρ_0^1) and the following weak solution. On the incoming arcs I_i there are waves with negative velocities connecting $\rho_{i,0}^1$ with $\bar{\rho}_{i,0}^2$, while on the outgoing arcs I_j there are waves with positive velocities connecting $\bar{\rho}_{j,0}^2$ with $\rho_{j,0}^1$. This is possible because all values are *good data*. At the vertex the datum is thus given by $\bar{\rho}^2$. This proves that this is a weak solution compatible with R1-3. The same happens inverting the roles of ρ_0^1 and ρ_0^2 . By contradiction, the proof is completed.

3.3.4 The Riemann Solver (R1-4)

This solver is entirely similar to solver R1-3 with the additional dependence on parameters Θ . Thus, reasoning as in the proof of Proposition 2.4 and 2.5 to have well-posed solutions, it is possible to restrict to the following rule:

(**Rule 4'**). The incoming flux is determined by:

$$\max_{\gamma_{in} \in V(\Theta) \cap \bar{\Omega}_{in}} \gamma_{in} \cdot (1, 1),$$

where $V(\Theta) = \{tv(\Theta) : t \in \mathbb{R}\}$, $\Theta \in \mathbb{R}^p$ represents some time-evolving parameters and $v : \mathbb{R}^2 \rightarrow \mathbb{R}^2$ is a fixed function.

The properties of such solver R1-4' are determined in a similar manner to those of R1-2.

3.3.5 The Riemann Solver (R2-1)

In this case we first determine the through flux Γ via (R2). Then, Rule (1) must be used on incoming arcs if $\Gamma < \Gamma_{in}$ and on outgoing ones if $\Gamma < \Gamma_{out}$. We set:

$$\Omega_{in}^\Gamma = \{\gamma_{in} \in \Omega_{in} : \gamma_1 + \gamma_2 \leq \Gamma\},$$

$$\Omega_{out}^\Gamma = \{\gamma_{out} \in \Omega_{out} : \gamma_3 + \gamma_4 \leq \Gamma\}.$$

In both cases the linear constraints used to determine the admissible region is orthogonal to the vector $(1, 1)$, thus we have:

Proposition 2.6: If v is not parallel to $(1, 1)$ then Rules (R2) and (1) determine a unique solution for every initial datum.

Again, if the assumption of proposition 2.6 does not hold then we can use Rule (C) taking v as priority vector. In this way the same conclusions as Proposition 2.2 holds.

3.3.6 The Riemann Solver (R2-2)

In this case it is necessary to proceed differently with respect to R2-1. In detail, if we first determine Γ and then use Rule (2) both for incoming and outgoing arcs, the respective solutions may violate (H2), thus the conservations of cars through the intersection.

For this reason, the strategy has to be inverted, namely:

- Firstly, Rule (2) is used both on incoming and outgoing arcs, then the through flux is obtained taking the minimum between the two.

In detail, γ^{-in} is defined by solving

$$\max_{\gamma_{in} \in V \cap \Omega_{in}} \gamma_{in} \cdot (1, 1)$$

and similarly γ^{-out} by solving

$$\max_{\gamma_{out} \in V \cap \Omega_{out}} \gamma_{out} \cdot (1, 1).$$

Then, the through flux is defined by

$$\Gamma = \min \{ \gamma_1^{-in} + \gamma_2^{-in}, \gamma_1^{-out} + \gamma_2^{-out} \}, \quad (2.4)$$

Finally, the solutions fluxes are given by

$$\hat{\gamma}_{in} = \Gamma \gamma^{-in}, \quad \hat{\gamma}_{out} = \Gamma \gamma^{-out}. \quad (2.5)$$

In other words, this solver is defined using first Rule (2) and then Rule (R2). It easy to check that this solver has the same properties of solver R1-2.

3.3.7 The Riemann Solver (R2-3)

In this case the steps are to first apply Rule (3) and then determine the through flux. However, the definition suffers from the same problems as for R1-3 both on incoming and outgoing arcs. In particular, Propositions 2.4 and 2.5 imply that a well-posed theory is possible only by reducing to case R2-2.

3.3.8 The Riemann Solver (R2-4)

This solver is entirely similar to solver 2-3 with the additional dependence on parameter Θ . We can proceed as for R2-2 by defining γ^{-in} as the solution of

$$\max_{\gamma_{in} \in V(\Theta) \cap \Omega_{in}} \gamma_{in} \cdot (1, 1)$$

and similarly γ^{-out} as the solution of

$$\max_{\gamma_{out} \in V(\Theta) \cap \Omega_{out}} \gamma_{out} \cdot (1, 1).$$

Then, it is possible to use (2.4) and (2.5) in order to define the solution fluxes. The properties of such solver are the same as those of solver R2-2.

3.4 Formulation of the Linear Programming Model for Riemann Solver

In this section, formulation of the linear programming model associated to Riemann problem is defined.

Model variables are:

- γ_i with $i \in \{1, \dots, n\}$, flux on incoming road i at the intersection J .
- γ_j with $j \in \{n + 1, \dots, n + m\}$, flux on outgoing road j at the intersection J .

- γ_i^{\max} with $i \in \{1, \dots, n\}$, maximum flux on incoming road i .
- γ_j^{\max} with $j \in \{n + 1, \dots, n + m\}$, maximum flux on outgoing road j .
- q_i with $i \in \{1, \dots, n\}$, coefficients relating to precedence which must be respected on the roads, such values are between 0 and 1.
- α_{ij} with $i \in \{1, \dots, n\}$ and $j \in \{n + 1, \dots, n + m\}$, coefficients that describe driver's preference. These coefficients state the traffic distribution from the incoming roads to outgoing ones and are defined in the *Distribution matrix* of the rule (A).

The *objective function* (*cost function*) maximizes the flux on incoming roads:

$$\max \sum_{i=1}^n \gamma_i.$$

The constraints of the problem can be divided into:

- *feasible region constraints*:

$$\begin{aligned} 0 &\leq \gamma_1 \leq \gamma_1^{\max} \\ &\dots \\ 0 &\leq \gamma_n \leq \gamma_n^{\max} \end{aligned}$$

- *distribution constraints*:

$$\begin{aligned} 0 &\leq \sum_{i=1}^n \alpha_{1i} \gamma_i \leq \gamma_1^{\max} \\ &\dots \\ 0 &\leq \sum_{i=1}^n \alpha_{mi} \gamma_i \leq \gamma_m^{\max}. \end{aligned}$$

If the number of incoming roads is greater than the number of outgoing ones, the rule of precedence (C) is also valid. Given a priority q_i associated with the road i , the *priority constraints* are:

$$\begin{aligned} \gamma_2 &= \frac{q_2}{q_1} \gamma_1 \\ \gamma_3 &= \frac{q_3}{q_1} \gamma_1 \\ &\dots \\ \gamma_n &= \frac{q_n}{q_1} \gamma_1 \end{aligned}$$

3.4.1 Assumptions for Alternative Riemann Solvers

About Rule (1) we assume the following condition:

- The *objective function (cost function)* maximizes the flux on incoming roads:

$$\max \sum_{i=1}^n v \cdot \gamma_i,$$

where v is the priority vector associated with the incoming road i for the intersection J .

About Rule (2) and Rule (3) we assume the following conditions:

- *feasible region constraints:*

$$\gamma_i = t \cdot v_i, \quad i \in [1, n] \quad (\text{by Rule (2)}). \quad (2.5)$$

Since $0 \leq \gamma_i \leq \gamma_i^{\max}$, deriving from Equation (2.5) we have that

$$\begin{aligned} t \cdot v_i &\leq \gamma_i^{\max}, \quad \text{i.e.} \\ t &\leq \frac{\gamma_i^{\max}}{v_i}, \quad i \in [1, n]. \end{aligned}$$

- *distribution constraints:*

$$\gamma_i = t \cdot v_i, \quad i \in [1, n] \quad (\text{by Rule (2)}). \quad (2.6)$$

Since $0 \leq \sum_{i=1}^n \alpha_{ji} \gamma_i \leq \gamma_i^{\max}$, deriving from Equation (2.6) we have

that

$$\begin{aligned} \sum_{i=1}^n \alpha_{ji} t \cdot v_i &\leq \gamma_i^{\max}, \quad \text{i.e.} \\ t &\leq \frac{\gamma_i^{\max}}{\sum_{i=1}^n \alpha_{ji} v_i}, \quad j \in [1, m]. \end{aligned}$$

- *priority constraints:*

$$\gamma_i = t \cdot v_i, i \in [1, n] \text{ (by Rule (2)).} \quad (2.7)$$

Since $\gamma_i = \frac{q_i}{q_1} \gamma_1$, deriving from Equation (2.7) we have that

$$\gamma_i = \frac{q_i}{q_1} t \cdot v_1, \text{ i.e.}$$

$$\gamma_i = q_i \cdot t$$

that is already satisfied by rule (2). For this reason, priority constraints for Rule (2) and Rule (3) are implicit.

Chapter 4

Numerical Schemes

Numerical methods are able to create an approximation of the exact solution and to evaluate the error committed by replacing the exact solution with the approximate one.

In this section, we will focus on some numerical methods for the discretization of the solution of non-linear hyperbolic equations (PDEs) about conservation laws modeling vehicular flux. In detail, we will describe one-dimensional case although most of the concepts and methods that we will introduce remain valid also for multi-dimensional case. We will pay specific attention to *Godunov* schema for the numeric solution of PDEs.

4.1 Approximations of non-linear hyperbolic problems

In this subsection we introduce some schemes for the discretization of the on-linear hyperbolic equations.

4.1.1 Approximation finite difference

Consider the hyperbolic equation

$$\frac{\partial \rho}{\partial t} + \frac{\partial}{\partial x} F(\rho) = 0, \quad t > 0, x \in \mathbb{R} \quad (3.1)$$

where F is a non-linear function of ρ , with the initial condition

$$\rho(x, 0) = \rho_0(x), \quad x \in \mathbb{R}.$$

In order to solve this equation numerically, we use discretization of space and time based on the finite difference method. The plane (x, t) is discretized by means of the choice of a step of constant time discretization $\Delta t = k$, and constant space discretization $\Delta x = h$ such that

$$\begin{cases} x_j = j \cdot h & j = 0, 1, \dots \\ x_{j+\frac{1}{2}} = x_j + \frac{h}{2} & j = 0, 1, \dots \\ t^n = nk & n = 0, 1, \dots \end{cases}$$

Therefore, in the plane (x, t) a *grid* is created by considering step of size h on axis x and step of size k on the axis t , as shown in Figure 4.1. We find discrete solutions ρ_j^n that approximate $\rho(x_j, t^n)$ for each spatial step j and temporal one n .

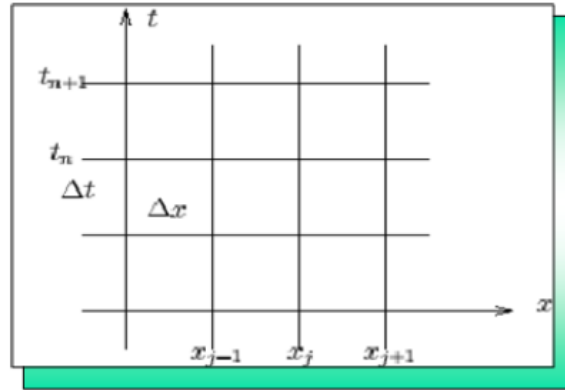


Figure 4.1 Grid

We use an explicit finite difference schema as follows:

$$\rho_j^{n+1} = \rho_j^n - \frac{\Delta t}{\Delta x} (H_{j+\frac{1}{2}}^n - H_{j-\frac{1}{2}}^n), \quad (3.2)$$

where $H_{j+\frac{1}{2}}^n = H(\rho_j^n, \rho_{j+1}^n)$, with $H(\cdot, \cdot)$ *numeric flux*.

Functional interpretation of the numerical flux is the follow

$$H_{j+\frac{1}{2}}^n \simeq \frac{1}{\Delta t} \int_{t^n}^{t^{n+1}} F(\rho(x_{j+\frac{1}{2}}, t)) dt,$$

that is $H_{j+\frac{1}{2}}^n$ approximates average flux by $x_{j+\frac{1}{2}}$ within time interval $[t^n, t^{n+1}]$. For a given numerical schema, truncation error τ_j^n at a point (x_j, t^n) is the error that is created by presuming that correct solution verify the same numeric schema. If the truncation error $\tau(\Delta t, h) = \max_{j,n} |\tau_j^n|$ tends towards zero when Δt and h independently tend towards zero then the numeric schema is called *consistent*.

The numeric flux must verify

$$H(\bar{\rho}, \bar{\rho}) = F(\bar{\rho}), \quad (3.3)$$

when $\bar{\rho}$ is a constant. Lax and Wendroff proved that, under the condition (3.3), the functions ρ such that

$$\rho(t^n, x_j) = \lim_{\Delta t, h \rightarrow 0} \rho_j^n$$

are *weak solutions* of initial problem. ρ is a weak solution of (3.1) if satisfy the differential relation (3.1) for all points $x \in \mathbb{R}$ except of those in which it is discontinuous. In these points it does not make sense that (3.1) is valid but it is important that *Rankine-Hugoniot* condition is verified:

$$F(\rho_r) - F(\rho_l) = \sigma(\rho_r - \rho_l),$$

where ρ_r and ρ_l state, respectively, right and left limit of ρ in the discontinuity point. The weak solutions are not necessarily unique. Among them, the weak solution pragmatically correct is the *entropic* one.

Unfortunately, the weak solutions are not entropic ones. In order to retrieve the entropic solutions, numeric schemas have to introduce an appropriate numeric diffusion.

Equation (3.2) can be re-written as

$$\rho_j^{n+1} = G(\rho_{j-1}^n, \rho_j^n, \rho_{j+1}^n). \quad (3.4)$$

Equation (3.4) has some characteristics:

- it is *monotonic* if G is an increasing monotonic function for each of its arguments;
- it is *limited* if $\exists C > 0$ such that $\sup_{j,n} |\rho_j^n| \leq C$;
- it is *fixed* if the finite difference solutions ρ^n and v^n derived from two different initial data ρ^0 and v^0 verify, $\forall n \geq 0$ such that $n\Delta t \leq T$ and $\forall \Delta t$ and h sufficiently small,

$$\|\rho^n - v^n\|_{\Delta} \leq C_T \|\rho^0 - v^0\|_{\Delta},$$

where $\|\cdot\|_{\Delta}$ is an appropriate discrete norm and the constant $C_T > 0$ is independent from Δt and h .

4.1.2 Approximation with discontinuous finite elements

An alternative approach to that adopted so far is based on the use of discontinuous finite element. This choice is motivated by the fact that the non-linear hyperbolic solutions may present problems of discontinuity even in the presence of continuous initial data. For the discretization of the problem (3.1) we now consider the spatial approximation based on discontinuous finite elements. We search $\forall t > 0 \rho_h(t) \in W_h$ where W_h represents finite elements space and such that we have $\forall j = 0, 1, \dots, m-1$ and $\forall v_h \in P_r(I_j)$ where $P_r(I_j)$ is space of Legendre polynomials

$$\int_{I_j} \frac{\partial v_h}{\partial t} v_h dx - \int_{I_j} F(\rho_h) \frac{\partial v_h}{\partial x} dx + H_{j+1}(\rho_h) v_h^-(x_{j+1}) - H_j(\rho_h) v_h^+(x_j) = 0, \quad (3.5)$$

where $I_j = [x_j, x_{j+1}]$. Initial datum ρ_h^0 is given by

$$\int_{I_j} \rho_h v_h dx = \int_{I_j} \rho^0 v_h dx \quad j = 0, 1, \dots, m-1.$$

Function H_j now denotes the non-linear numeric flux in point x_j and depends on values u_h and x_j , that is

$$H_j(\rho_h(t)) = H_j(\rho_h^-(x_j, t), \rho_h^+(x_j, t)).$$

If $j = 0$, it is necessary to put $\rho_h^-(x_0, t) = \phi(t)$, that is the datum on board in the left end (supposing, of course, this is inflow point).

We observe that there are various possibilities of choice for the function H . However, we want that these choices generate, by (3.5), *monotonic* schemas that are stable and converge to the entropic solution. In detail, we want that (3.5) is a monotonic schema when $r = 0$ (r is the degree of Legendre polynomial).

In this case $\int_{I_j} F(\rho_h) \frac{\partial v_h}{\partial x} = 0$ because being null the degree r of Legendre polynomial v_h , this will be constant and its derivative with respect to x is null.

Then, if $\rho_h^{(j)}$ is the constant value of ρ_h on I_j , Equation (3.5) becomes

$$h_j \frac{\partial}{\partial t} \rho_h^{(j)}(t) + H(\rho_h^{(j)}(t), \rho_h^{(j+1)}(t)) - H(\rho_h^{(j-1)}(t), \rho_h^{(j)}(t)) = 0 \quad (3.6)$$

with initial datum $\rho_h^{0,(j)} = h_j^{-1} \int_{x_j}^{x_{j+1}} \rho_0 dx$ within the interval I_j , $j = 0, 1, \dots, m-1$ by having indicated with $h_j = x_{j+1} - x_j$ the size of I_j .

In order that schema (3.6) is monotonic the flux H must be monotonic.

Some examples of monotonic flux are described below.

- **Godunov flux**

$$H(v, w) = \begin{cases} \min_{v \leq \rho \leq w} F(\rho) & \text{if } v \leq w \\ \max_{w \leq \rho \leq v} F(\rho) & \text{if } v > w \end{cases}$$

- **Engquist-Osher flux**

$$H(v, w) = \int_0^v \max(F'(\rho), 0) du + \int_0^w \min(F'(\rho), 0) du + F(0).$$

- **Lax-Friedrichs flux**

$$H(v, w) = \frac{1}{2} [F(v) + F(w) - \delta(w - v)],$$

$$\delta = \max_{\inf_x \rho_0(x) \leq \rho \leq \sup_x \rho_0(x)} |F'(\rho)|$$

Godunov flux generates the least amount of numeric dissipation.

4.2 Numerical methods for vehicular traffic networks

Numeric method for the vehicular traffic network model described in Chapter 3 is designed by a generalization of the class of finite difference methods defined for non-linear problems.

This numeric scheme:

- reflects the conservative nature of the initial problem;
- is influenced by the direction of the flux function: in fact, the problem we are analyzing has a preferential spatial direction in time; we want that by numerically solving the problem, the approximate solution is created according to significant density values relating to earlier instants of time;
- has numeric properties such as consistency, solidity and convergence; these properties ensure that the approximate solution, starting from any initial data, is limited and free from oscillations.

Godunov numeric method is the most appropriate one for the discretization of the law of conservation at the base of the model referred to above.

4.2.1 Godunov method

The Godunov method was introduced in 1959 for the resolution of the Euler equation about dynamic gas in the presence of shock waves [17]. It is based on the solution of local Riemann problems. The idea is to solve the problem at each time interval in each cell of the spatial grid by separately treating a sequence of Riemann problems.

In general, (unique) solution of the Riemann problem

$$\rho_t + f(\rho)_x = 0, \quad x \in \mathbb{R}, \quad t \in [0, 1]$$

with initial datum

$$\rho(x, 0) = \rho_0(x) = \begin{cases} \rho_l & \text{if } x < 0 \\ \rho_r & \text{if } x > 0 \end{cases}$$

is self-similar, that is

$$\rho(x, t) = W_R\left(\frac{x}{t}; \rho_l, \rho_r\right),$$

where W_R depends only on function flux F and it is composed of two constant states ρ_l and ρ_r , that are separated by different waves departing from the source and whose speeds are limited by

$$\max \{|F(\xi)|, \xi \text{ between } \rho_l \text{ and } \rho_r\}.$$

We search for an approximate solution of this problem.

We assign an initial datum $\rho_0(x)$ and approximate it by v^Δ representing a constant function sometimes defined in $\mathbb{R} \times (0, +\infty)$.

First step

The initial datum is approximate by sequence $v^0 = (v_m^0)$ as follows:

$$v_m^0 = \frac{1}{\Delta x} \int_{x_{m-\frac{1}{2}}}^{x_{m+\frac{1}{2}}} \rho_0(x) dx.$$

We define function v^Δ as

$$v_0^\Delta(x) = v_m^0, \quad x \in (x_{m-\frac{1}{2}}, x_{m+\frac{1}{2}}), m \in \mathbb{Z}.$$

Similarly, given an approximation v_m^n of ρ at time $t = t_n$ we set

$$v^\Delta(x, t_n) = v_m^n, \quad x \in (x_{m-\frac{1}{2}}, x_{m+\frac{1}{2}}), m \in \mathbb{Z}.$$

This schema defines v_m^n recursively starting from v_m^0 . $v^\Delta(x, t_n)$ is the solution of the problem

$$\begin{cases} \partial_t v + \partial_x F(v) = 0 \\ v(x, t_n) = v^\Delta(x, t_n) \end{cases} \quad x \in \mathbb{R}, \quad t \in (t_n, t_{n+1}).$$

Since v^Δ is part of $L^\infty(\mathbb{R})$ (space of limited functions almost everywhere on \mathbb{R}), the problem has a unique entropic solution that can be determined explicitly at least for Δt small enough.

Notice that if

$$\Delta t \sup_{m,n} \left\{ \sup_{u \in I(u_m^n, u_{m+1}^n)} |F(\rho)| \right\} \leq \frac{1}{2} \Delta x$$

a wave starting from $x_{m-\frac{1}{2}}$ will not reach straight lines $x = x_{m-1}$ and $x = x_m$ before time t_{n+1} .

Second step

We define

$$v_m^{n+1} = \frac{1}{\Delta x} \int_{x_{m-\frac{1}{2}}}^{x_{m+\frac{1}{2}}} v^\Delta(x, t_{n+1}) dx \quad (3.8)$$

that represents the projection of the correct solution on a constant interval function.

In order to get a simple expression for v_m^{n+1} , we use Gauss-Green formula to integrate Equation (3.8) on cell $(x_{m-\frac{1}{2}}, x_{m+\frac{1}{2}}) \times (0, \Delta t)$.

This is possible because ρ is a constant interval function and satisfy Rankine - Hugoniot condition at discontinuity. We have that

$$0 = \int_{t_n}^{t_{n+1}} \int_{x_{m-\frac{1}{2}}}^{x_{m+\frac{1}{2}}} (\partial_t v + \partial_x F(v)) dx dt = \int_{x_{m-\frac{1}{2}}}^{x_{m+\frac{1}{2}}} [v(x, t_{n+1}) - v(x, t_n)] dx + \int_{t_n}^{t_{n+1}} [F(v(x_{m-\frac{1}{2}}, t)) - F(v(x_{m+\frac{1}{2}}, t))] dt.$$

A precondition for solidity of a numeric schema is that temporal and spatial discretization step are linked together by the following relation:

$$\Delta t \leq \frac{\Delta x}{|a|}$$

that is called *CFL* condition (by Courant, Friedrichs and Lewy) and associated number (adimensional because a is a velocity) is called *CFL number*.

Under CFL condition

$$\Delta t \sup_{m,n} \left\{ \sup_{u \in I(u_m^n, u_{m+1}^n)} |F(\rho)| \right\} \leq \Delta x, \quad (3.9)$$

waves do not affect solution in $x = x_{m+\frac{1}{2}}$, for $t \in (t_n, t_{n+1})$. Then, solutions are locally given by Riemann problems and flux in $x = x_{m+\frac{1}{2}}$, for $t \in (t_n, t_{n+1})$ is given by

$$F(\rho(x_m, t)) = F(W_R(0; v_{m-1}^n, v_m^n)).$$

Since the flux is invariant according to time and continuous, we can extract it from integral sign and obtain

$$v_m^{n+1} = v_m^n - \frac{\Delta t}{\Delta x} (F(W_R(0; v_m^n, v_{m+1}^n)) - F(W_R(0; v_{m-1}^n, v_m^n))).$$

We have that

$$g^G(\rho, v) = F(W_R(0; \rho, v))$$

so that numeric flux g^G has expression

$$g^G(\rho, v) = \begin{cases} \min_{w \in [\rho, v]} F(w) & \text{if } \rho \leq v \\ \max_{w \in (\rho, v)} F(w) & \text{if } v \leq \rho \end{cases}$$

For specific case of this dissertation Godunov numeric flux is the following:

$$g^G(\rho, v) = \begin{cases} \min(F(\rho), F(v)) & \text{if } \rho \leq v \\ F(\rho) & \text{if } v < \rho < \sigma \\ F(\sigma) & \text{if } v < \sigma < \rho \\ F(v) & \text{if } \sigma < v < \rho \end{cases}$$

where σ depends on max of flux function F .

This schema, under condition (3.9) can be write as follows:

$$v_m^{n+1} = v_m^n - \frac{\Delta t}{\Delta x} (g^G(v_m^n, v_m^{n+1}) - g^G(v_{m-1}^n, v_m^n)).$$

Boundary conditions

We suppose to assign a condition type to boundary $x = 0$:

$$\rho(0, t) = \rho_b(t), \quad t > 0$$

and want to study equation only for $x > 0$.

We consider the problem

$$\begin{cases} \rho_t + f(\rho)_x = 0 & x \in I, t \in [0, T] \\ \rho(x, 0) = \rho_0(x) & x \in I \\ \rho_x(0, t) = \rho_b(t) & t \in [0, T] \end{cases}$$

where I is an open interval within R , $\rho_0 \in C^1(I)$, $\rho_1(t) \in C^1(0, T)$, $F \in C^1(R)$.

It is not easy to find a function that satisfies the problem in the classical sense, because in general you can not assume boundary data. For example, we consider scalar problem

$$\begin{cases} \rho_t - \rho_x = 0 & R^+ \times (0, T) \\ \rho(x, 0) = \rho_0(x) & R^+ \times \{0\} \end{cases}$$

This problem has a unique global solution $\rho(x, t) = \rho_0(x + t)$ within $(0, +\infty) \times (0, +\infty)$, so condition

$$\rho(0, t) = \rho_b(t), \quad t \geq 0 \quad (3.10)$$

is not consistent. On the other hand, for problem

$$\begin{cases} \rho_t + \rho_x = 0 & R^+ \times (0, T) \\ \rho(x, 0) = \rho_0(x) & R^+ \times \{0\} \end{cases}$$

is necessary that condition (3.10) is set up. From previous example, it is obvious that the need to assign a boundary condition is related to the function flux. For example, the boundary condition is applied when $F'(\rho_b) > 0$ [2].

Then, we have

$$\rho(0, t) = \rho_b(t)$$

only for t values such that $F'(\rho(0, t)) > 0$.

In detail, we proceed by inserting a ghost cell and defining

$$v_0^{n+1} = v_0^n - \frac{\Delta t}{\Delta x} (g^G(v_0^n, v_1^n) - g^G(\rho_1^n, v_0^n)),$$

where

$$\rho_1^n(t) = \frac{1}{\Delta t} \int_{t_n}^{t_{n+1}} \rho_b(t) dt$$

replaces v_{-1}^n .

A boundary datum outgoing can be considered in a similar way. Suppose $x < L = x_N$. Then, formal condition is given by

$$\rho(L, t) = \rho_2(t)$$

so we have

$$v_N^{n+1} = v_N^n - \frac{\Delta t}{\Delta x} (g^G(v_N^n, \rho_2^n) - g^G(v_{N-1}^n, v_N^n)),$$

where

$$\rho_2^n(t) = \frac{1}{\Delta t} \int_{t_n}^{t_{n+1}} \rho_2(t) dt$$

replaces v_{N+1}^n that is a value of ghost cell.

Conditions at intersections

For incoming arcs into a node, we set:

$$v_N^{n+1} = v_N^n - \frac{\Delta t}{\Delta x} (\gamma_i - g^G(v_{N-1}^n, v_N^n))$$

while for outgoing arcs we have that:

$$v_0^{n+1} = v_0^n - \frac{\Delta t}{\Delta x} (g^G(v_0^n, v_1^n) - \gamma_j),$$

where γ_i and γ_j are maximized fluxes (computed by Riemann Solver described in Chapter 3) and subindices i and j indicates respectively incoming and outgoing arcs.

Chapter 5

Experimentation and Numerical Results

Main goal of this section is to analyze a real case study representing a road network by simulating traffic flows with different models based on Riemann Solver described in Chapter 3, for realizing if it is possible to contribute to the improvement of network viability by suggesting some different planning activities. The models used for experimentation are **RS Base**, **RS 1** and **RS 2**.

5.1 Operating Specifications

In order to analyze the vehicular traffic behaviour on a road network by simulating it through the three different models and achieve the main objectives, it is important to configure topological characteristics of the network and define proper initial conditions.

5.1.1 Configuration parameters

The road network is constituted of a **node set** corresponding to **intersections** and a **directed arc set** representing the **roads**.

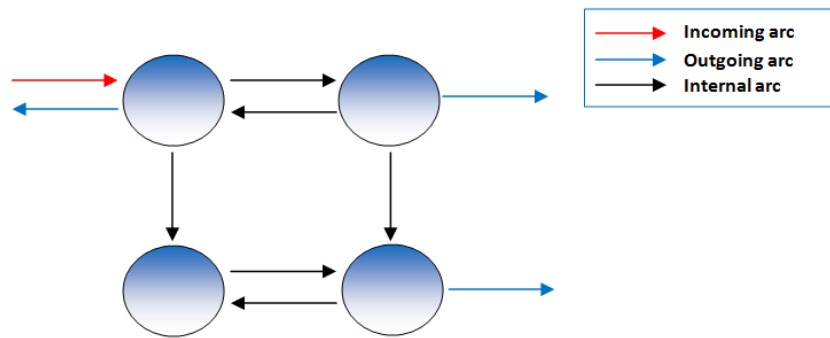


Figure 5.1 Road Network Graph

In detail, there are three types of arc, as shown in Figure 5.1:

- *Incoming arc*: it represents the incoming road into an intersection.
- *Outgoing arc*: it represents the outgoing road from an intersection.
- *Internal arc*: it represents the road between two active intersections.

In addition, each arc is characterized by the following properties:

- *Node pair* (or *single node* for incoming or outgoing arcs, in which case one extreme is ideally infinity) identifying the intersections in which the arc is incoming or from which it is coming out.
- *Direction* (being directed arcs) identifying the way of the vehicular flux.
- *Length* identifying largeness of the roads.

5.1.2 Input data

Simulation requires the following input data:

- **Intersection activation:** what are the incoming roads into the intersection and what are the outgoing roads from intersection.
- **Initial density** (of the vehicles) along all network arches (roads).
- **Boundary data:** if the incoming (or outgoing) road i has an extreme infinity, it is necessary to indicate a hypothetical density along the road as boundary datum ($\rho_{i,b}$ with $b = \infty$).
- **Maximum velocity** v_{\max} and **maximum density** ρ_{\max} (of the vehicles) if a *parable* function flux is used on the arc, given by:

$$f(\rho) = v_{\max} \cdot \rho \cdot \left(1 - \frac{\rho}{\rho_{\max}}\right)$$

or **maximum flux** γ_{\max} , **maximum density** ρ_{\max} and **sigma** σ (of vehicles) if a *pulldown* function flux is used on the arc, given by:

$$f(\rho) = \begin{cases} \frac{\gamma_{\max}}{\sigma} \cdot \rho & \text{if } 0 \leq \rho \leq \sigma \\ \frac{(\sigma - \rho_{\max}) \cdot (\rho - \sigma)}{\gamma_{\max}} + \gamma_{\max} & \text{if } \sigma < \rho \leq \rho_{\max} \end{cases}$$

- **Distribution coefficients** $\alpha_{i,j}$ between 0 and 1 on incoming and outgoing arches for each $n \times m$ node with $n \leq m$, representing the percentage of flux that from the incoming road i goes to the outgoing road j . For example, Figure 5.2 shows how the incoming flux into the node from the unique incoming road is distributed to the 70% on the road 2 and to 30% on the road 3.

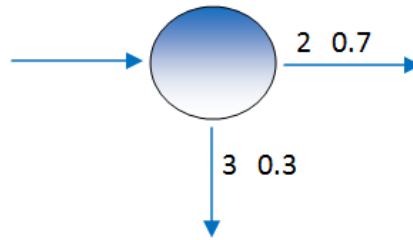


Figure 5.2 Distribution coefficients

- **Priority** q_i for $n \times m$ nodes with $n \geq m$, representing the percentage of flux incoming into the node (intersection) from the arch (road) i (see Figure 5.3).

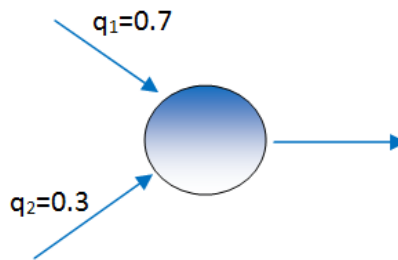


Figure 5.3 Priority

- **Temporal parameters:** total duration of the simulation (T), size of the spatial discretization step (Δx) and size of the temporal discretization step (Δt).
- **Riemann Solver Model:** choice of the Riemann Solver Model through which run the simulation. The possible choices are **Base Riemann Solver (RS Base)**, **Alternative Riemann Solver 1 (RS 1)** and **Alternative Riemann Solver 2 (RS 2)**.

Figure 5.4 shows an example for the correct configuration of the input parameters within the software simulator.

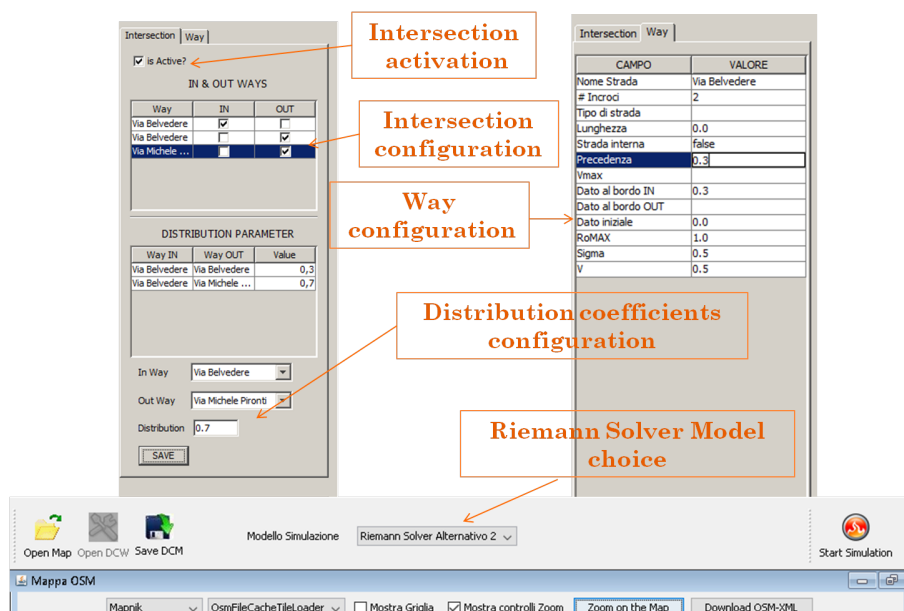


Figure 5.4 Example of Simulator Configuration

5.1.3 Output data

The output resulting from the simulation is the estimated traffic density on each discretized road of the network at any instant of time on the whole duration of the simulation.

5.2 Case Study

Figure 5.5 shows the real road network considered for the simulation of traffic flow whose information are derived by an OSM map¹. It represents a specific area of Salerno city constituted of roads and appropriate intersections.

¹OpenStreetMap is a collaborative project to create a free editable map of the world. <https://www.openstreetmap.org>

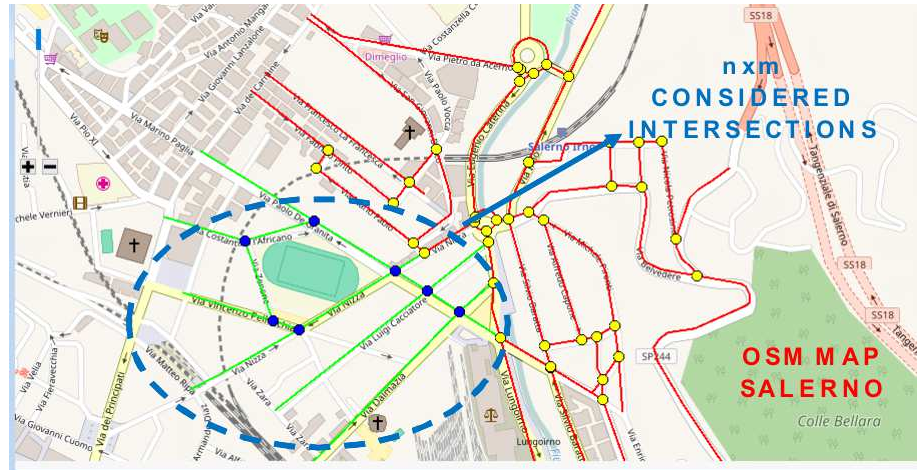


Figure 5.5 OSM Map of Salerno city

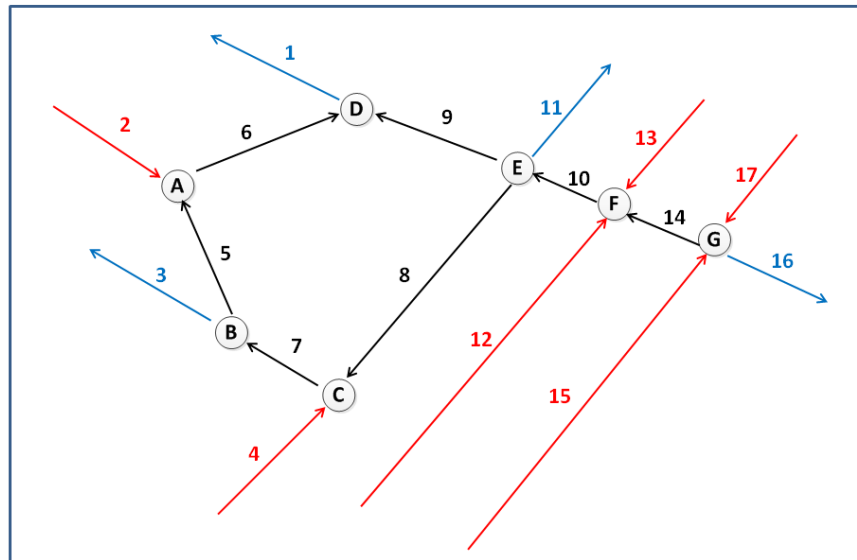


Figure 5.6 Case study - Road network

In detail, Figure 5.6 shows the topology of the graph representing the road network of Figure 5.5 which consists of **seven nodes** (from **A** to **G** representing the **intersections**) and **seventeen directed arcs** (from **1** to **17** representing the **roads**).

Table 5.1 lists information about the numbered roads of Figure 5.6. The specific information is:

- **ID**: increasing numerical character identifying a specific road of the network.
- **Name**: name associated with the road.
- **Length**: road length measured in meters.
- **Internal road**: flag value identifying if a specific road is an internal road or not.

ID	Name	Length (meters)	Internal road
1	Via Paolo De Granita	240	No
2	Via Costantino l'Africano	140	No
3	Via Vincenzo Pellecchia	140	No
4	Via Nizza	200	No
5	Via Zenone	140	Yes
6	Via Costantino l'Africano	130	Yes
7	Via Vincenzo Pellecchia	90	Yes
8	Via Nizza	190	Yes
9	Via Paolo De Granita	170	Yes
10	Via Giovanni Francesco Memoli	70	Yes
11	Via Nizza	70	No
12	Via Luigi Cacciatore	350	No
13	Via Luigi Cacciatore	150	No
14	Via Giovanni Francesco Memoli	80	Yes
15	Via Dalmazia	400	No
16	Via Dalmazia	70	No
17	Via Francesco Farao	80	No

Table 5.1 Case study - List of roads

Table 5.2 lists information about the intersections labeled with alphabetic characters of Figure 5.6. The information is:

- **ID**: alphabetic character identifying a specific intersection.
- **Typology**: $n \times m$ structure identifying a specific intersection where n represents the number of incoming roads and m represents the number of outgoing roads.
- **Incoming road ID**: list of the IDs associated with the incoming roads into a specific intersection.
- **Outgoing road ID**: list of the IDs associated with the outgoing roads from a specific intersection.

ID	Typology	Incoming road ID	Outgoing road ID
A	2×1	2, 5	6
B	1×2	7	3, 5
C	2×1	4, 8	7
D	2×1	6, 9	1
E	1×3	10	8, 9, 11
F	3×1	12, 13, 14	10
G	2×2	15, 17	14, 16

Table 5.2 Case study - List of intersections

For the experimentation we choose a *parable* function flux on all roads and, for this reason, we set the following parameters: $\rho_{\max} = 1$, $\sigma = 0.5$, $v_{\max} = 0.5$, $\gamma_{\max} = 0.5$. We also consider all roads initially empty (i.e. $\rho_0 = 0.0$).

The network is so configured:

- For each **incoming road** of the network (**red lines** in the graph of Figure 5.6): $\rho_{i,b} = 0.3$, for $i = 2, 4, 12, 13, 15, 17$.
- For each **outgoing road** of the network (**blue lines** in the graph of figure 5.6): $\rho_{j,b} = 0.3$, for $j = 1, 3, 11, 16$.

- For each **internal road** of the network (**black lines** in the graph of Figure 5.6) there is no boundary data.
- **Distribution** and **priority coefficients** for any single intersection are:

Intersection A: 2×1 junction with distribution matrix $A = (1, 1)$ and priorities $q_2 = 0.7$ and $q_5 = 0.3$.

Intersection B: 1×2 junction with distribution matrix $A = \begin{pmatrix} 0.5 \\ 0.5 \end{pmatrix}$ and no priority (i.e. $q_7 = 1$).

Intersection C: 2×1 junction with distribution matrix $A = (1, 1)$ and priorities $q_4 = 0.7$ and $q_8 = 0.3$.

Intersection D: 2×1 junction with distribution matrix $A = (1, 1)$ and priorities $q_6 = 0.7$ and $q_9 = 0.3$.

Intersection E: 1×3 junction with distribution matrix $A = \begin{pmatrix} 0.34 \\ 0.33 \\ 0.33 \end{pmatrix}$ and no priority (i.e. $q_{10} = 1$).

Intersection F: 3×1 junction with distribution matrix $A = (1, 1, 1)$ and priorities $q_{12} = 0.5$, $q_{13} = 0.3$ and $q_{14} = 0.2$.

Intersection G: 2×2 junction with distribution matrix $A = \begin{pmatrix} 0.5 & 0.5 \\ 0.5 & 0.5 \end{pmatrix}$ and priorities $q_{15} = 0.7$ and $q_{17} = 0.3$.

For the experimentation, we consider the length of each road as normalized, a simulation time interval $[0, T]$, with $T=60$ (which represents a time horizon of observation) and a numerical grid with $\Delta x=0.125$, $\Delta t = CFL \times \Delta x$ where $CFL=1$. The number of discrete time instants is given by the ratio $\frac{T}{\Delta t}=480$ and accordingly the time variable t is referred to these instants.

5.3 Experimentation results

This section shows the numerical results obtained by simulating traffic flows on the road network designed for the case study described in previous section.

So that the results of the experimentation can be useful for understanding the type of intervention to be implemented along the road network in order to improve driveability, it was necessary to analyze different situations by considering the main characteristics of each model based on Riemann Solver (i.e. RS Base, RS 1 and RS 2) used for the simulations.

Summarizing some outputs resulted from Chapter 3, RS Base models behaviour of vehicular flow across intersections by no simulating traffic lights. Differently, both RS 1 and RS 2 simulate behaviour of vehicular flow across intersections by simulating traffic lights at each intersection, where the first models traffic lights having a variable schedule of red-green times while the second one models a light with a fixed schedule.

Experimentation activities carried out were:

1. Simulation on the road network of vehicular flow by running in the order RS base, RS 1 and RS 2 and their graphical comparison on some different typologies of intersections. Goal of this activity was to highlight what approach (i.e. presence or absence of traffic lights) could have been improved any congestion situations by observing car densities.
2. Where it was necessary to have traffic lights at intersections to optimize road traffic, we analyzed a typology of intersection where there was high congestion for evaluating how to locally optimize the driveability by modifying the traffic light cycle time, also assessing the impact on the entire network.

About **Activity 1**, for each incoming and outgoing road of the intersections of the road network, a comparison graph among adopted models highlighting cars density is presented.

Let's consider $n \times m$ intersection where n is the number of incoming roads into the intersection and m is the number of outgoing roads from intersection.

We analyzed behaviour of the simulation according to the different models for the two most meaningful classes of $n \times m$ intersections in the road network:

1. intersection with $n < m$ and $n=1$;
2. intersection with $n > m$ and $m=1$.

About **class 1**, being a single entry road at the intersection, the presence of traffic lights is to be considered null as it is necessary for cars to travel that road. For this reason, RS base is the only model that can correctly simulate situations of this type. We refer figures from 5.7 to 5.9 showing the results of the simulation of RS Base for the Intersection B (1×2 intersection).

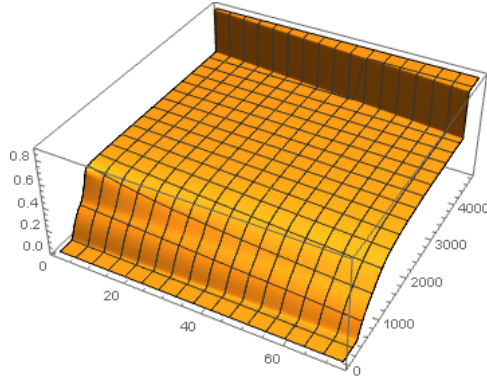


Figure 5.7 Intersection B - Incoming Road ID7

Figure 5.7 shows the simulated behaviour of RS Base for the incoming road (ID7) of the intersection.

At $t=0$, having assumed that the road is empty density values are all 0.0, then slowly increase to a fairly high value (>0.8) suggesting a bit of slowdown close to the intersection due to the need of traveling along one of the two outgoing roads according to distribution coefficients.

Figure 5.8 shows the simulated behaviour of RS Base for the first outgoing road (ID3) of the intersection.

Notice that cars flow along the road according to the distribution coefficients for the intersection B. Flux is evenly distributed with the second outgoing road (ID 5) of the intersection because both roads have the same probability (i.e. same distribution coefficient equal to 0.5) to be crossed by cars.

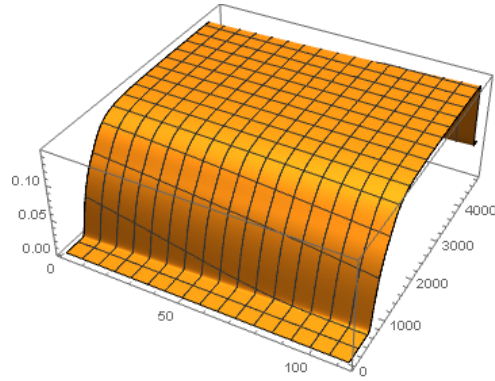


Figure 5.8 Intersection B - Outgoing Road ID3

Density values increase slowly with the aim of reaching a regime value that does not exceed outgoing boundary one ($=0.3$) since the road has an infinite extremity. Toward the end of the overall duration of the simulation, RS Base predicts lower density values due to the definition of the model according to which the road does not have a significant importance (i.e. priority is 0).

Figure 5.9 shows the simulated behaviour of RS Base for the second outgoing road (ID5) of the intersection.

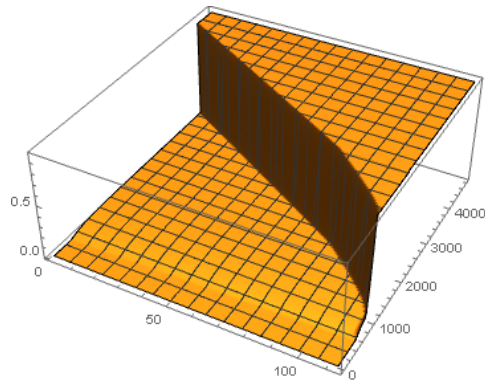


Figure 5.9 Intersection B - Outgoing Road ID5

At first, the model predicts low density values (<0.2), that are

constant for a certain period of time, resulting from distribution of cars flux along the road according to the specific coefficients.

Subsequently, towards the end of the overall duration of the simulation it is noticed as density values increase since the cars are reaching a new intersection (Intersection C). A congestion situation occurs because the road has low relevance (priority is 0.3), then cars coming from the others incoming roads (i.e. road with ID2 where priority is equal to 0.7) will cross the Intersection C first.

About **class 2**, we refer figures from 5.10 to 5.12 showing the results of the simulation of RS Base, RS 1 and RS 2 for the Intersection A (2×1 intersection).

Graph legend is explained as follows. *Graph x-axes* represents time instants while *graph y-axes* represents estimated density of vehicles on road crossing the intersection. *Blue color line* represents the estimated density of vehicles on the road according to RS Base. *Violet color line* represents the estimated density of vehicles on the road according to Alternative Riemann Solver 1 (RS 1), while *mustard color line* represents the estimated density of vehicles on the road according to Alternative Riemann Solver 2 (RS 2).

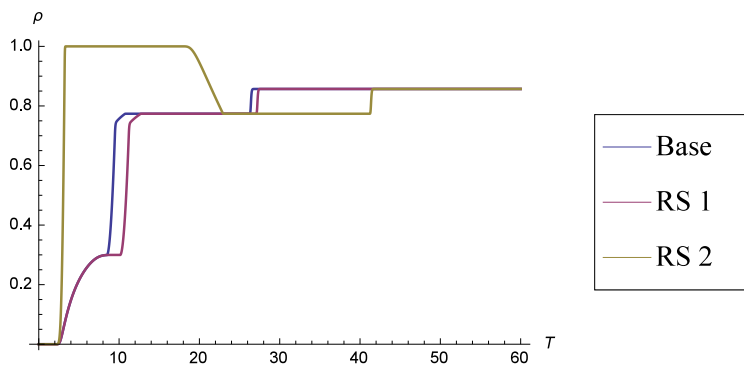


Figure 5.10 Intersection A - Incoming Road ID2

Figure 5.10 shows the simulated behaviour of the three models

for the first incoming road (ID2) of the intersection.

It is highlighted as modeling of absence of traffic lights provided by RS Base does not seem an optimal solution because density values are higher than those resulting from RS 1 and RS 2 that model presence of the traffic lights.

About RS 1, at $t=0$ density values are all 0.0 because we considered empty road but, subsequently, they correctly lowly increase until to reach incoming boundary datum value ($=0.3$) because the road has an infinite extremity. Also, density values of RS 1 change along the time because it models the behaviour of a traffic light with a variable schedule of red-green times. Near the intersection (at the end of the overall duration of the simulation), density values have a uniform distribution (>0.8 , and a little congestion state occurs) resulting also by considering importance of the road (priority is 0.7).

Notice that RS 2 has a very high car density at the beginning of simulation (with a consequent presence of congestion) due to incoming cars' densities (according to boundary datum value) and fixed schedule of red-green times of the traffic light resulting from the behaviour of the model. In the following time instants, density values have a uniform distribution resulting from the switch from red to green (and vice versa).

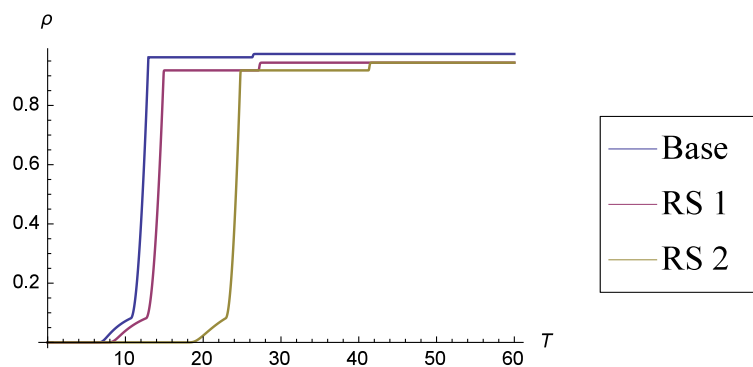


Figure 5.11 Intersection A - Incoming Road ID5

Figure 5.11 shows the simulated behaviour of the three models

for the second incoming road (ID5) of the intersection.

Also in this case, modeling of absence of traffic lights provided by RS Base does not seem an optimal solution because density values are higher than those resulting from RS 1 and RS 2 that model presence of the traffic lights.

Both for RS 1 and RS 2, at $t=0$ density values are all 0.0 because the road is considered empty but at following time instances they increase reaching a steady state with higher values (>0.9) and causing a congestion state. It is correct that these values are higher than those of road ID2 because road ID5 is less important than road ID2 (i.e. priority is more less, 0.3 for ID5 and 0.7 for ID2).

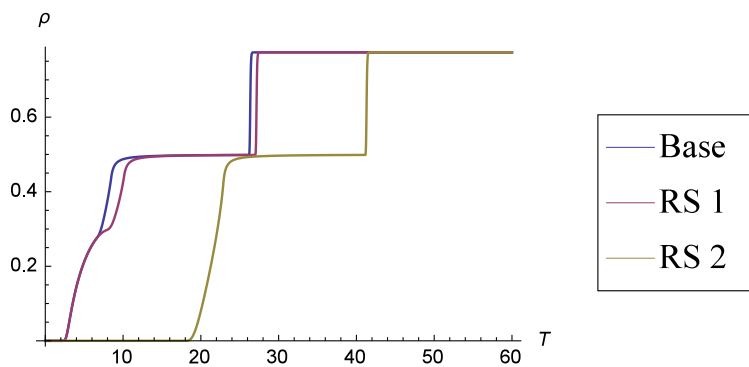


Figure 5.12 Intersection A - Outgoing Road ID6

Figure 5.12 shows the simulated behaviour of the three models for the outgoing road (ID6) of the intersection.

For each model, density values spread out according to distribution coefficients of matrix A and increase slowly reaching a steady state with lower values (>0.7) compared to those of road ID9 (>0.9) due its major relevance (priority is 0.7, while for road ID9 it is 0.3). In fact, road ID6 and road ID9 are incoming for the Intersection D of the road network.

From the execution of Activity 1 and from the consequent results obtained, we deduced a double consideration:

- RS Base can be used to correctly simulate traffic flow across $1 \times m$ intersections because the presence of traffic lights on the unique incoming road is irrelevant.
- About $n \times m$ intersections, RS 1 and RS 2 seem to be the most appropriate solutions for modelling this typology of intersection by providing traffic lights with variable or fixed schedule of red-green times. The optimal solution would be installation of traffic lights on intersections with sensors measuring continuously cars' densities in real-time and adapt in a variable way the schedule of red-green times (and so RS 1 could be useful for simulating traffic flow by adjusting road parameters). But, in the real situations of everyday life often this is not possible due to different problems such as lack of funds or difficulty in managing sensors equipment. For this reason, the solution is limited to adoption of traffic lights which have to be adequately temporized (and so RS 2 could be useful for simulating traffic flow) in order to optimize car traffic by reducing or, if possible, avoiding congestion states. This last consideration was the input for the following Activity 2 of experimentation.

About **Activity 2**, the goal of experimentation was to analyze a specific intersection of the road network in order to evaluate how it would be possible optimize car traffic at intersection by regulating behaviour of vehicular flux through the choice of appropriate schedule of red-green cycles for traffic lights arranged at intersection. This evaluation was carried out by simulating vehicular flow on the road network through RS 2 model and a 2×1 intersection was considered.

Let be A and B the two incoming roads and C the outgoing one of the intersection. The traffic light, in a generic time instant, is red for a road and green for the other. In particular, if drivers for road A see the red phase, then drivers of road B can be circulate. Hence, road A is characterized by a null priority while road B has a priority equal to 1. On the contrary, if drivers for

road A see the green phase, they can circulate. Suppose that the optimization procedure establishes that, from the road A a given percentage of traffic flux, q , should go the outgoing road. In this case, an adequate temporization of traffic light cycles is necessary. In particular, let Δ_v , Δ_r , and $T = \Delta_v + \Delta_r$ be, respectively, the green time, the red one and the complete traffic light cycle. In this case, as q represents the percentage of drivers who, from road A , must cross the intersection on average, then such parameter can be interpreted as the ratio among the green cycle and the total traffic light cycle. For this reason, the road B is characterized by an averaged priority equal to $1 - q$, or the ratio among the red cycle and the total cycle time. As a consequence, if q is the optimal road priority, it is useful to design the traffic cycles such that $\Delta_v = qT$ and $\Delta_r = (1-q)T$.

Intersection A with incoming roads ID2 and ID5 and outgoing road ID6 was analyzed. Figures 5.13 and 5.14 show the simulated behaviour of RS 2 on the two incoming roads with initial parameters configured for the road network of case study.

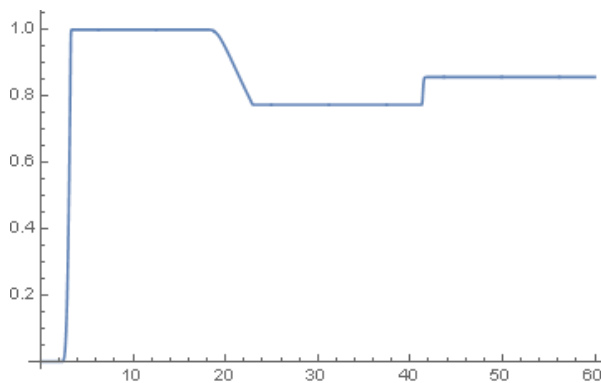


Figure 5.13 Intersection A - Incoming Road ID2 - RS 2 Simulation

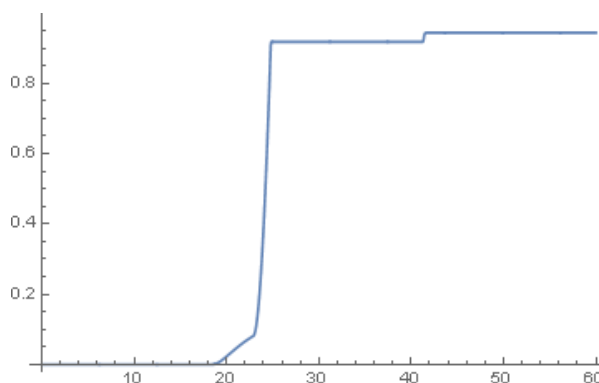


Figure 5.14 Intersection A - Incoming Road ID5 - RS 2 Simulation

As we can see, both figures highlight the correctness of RS 2 model. In fact, for example in the first time interval $[0,20]$, we notice as the traffic light simulated is green for road ID5 and red for road ID2 with consequent increase of vehicular densities for road ID2 and decrease for road ID5. Otherwise, for example in the time interval $[20,40]$ we notice as the traffic light is red for road ID5 and green for ID2, so we can conclude that RS 2 model behaves as we expect.

In addition, a congestion state occurs at the intersection. In order to evaluate how to optimize car traffic across the intersection for decreasing the congestion, we compared different choices for red-green cycles of traffic light trying to analyze what solution would be the most appropriate also observing the impact on the other roads of the network.

We simulated vehicular traffic with RS 2 model by assigned three new priority pairs on the incoming roads (ID2 and ID5) of the intersection A, different from the pair firstly assigned in the road network configuration (Priority for road ID2 is equal to 0.7 and priority for road ID5 is equal to 0.3, as shown in Figures 5.13 and 5.14). In this way, basing on previous considerations about traffic light for 2×1 intersections, we obtained three different red-green cycles for the traffic light.

In detail, we chose the following priorities q_i , for $i=2,5$:

1. $q_2 = 0.8$ and $q_5 = 0.2$;
2. $q_2 = 0.5$ and $q_5 = 0.5$;
3. $q_2 = 0.3$ and $q_5 = 0.7$;

Figures 5.15 and 5.16 show vehicular flow on the two incoming roads of the intersection (ID2 and ID5) with the chosen priorities.

Graph legend is explained as follows. *Graph x-axes* represents time instants while *graph y-axes* represents estimated density of vehicles on road crossing the intersection. *Blue color line* represents the estimated density of vehicles on the road according to roads' priorities and this is equivalent to a longer green cycle of the traffic light for road ID5 and shorter for road ID2. *Orange color line* represents the estimated density of vehicles on the road according to roads' priorities and this is equivalent to an equal green cycle of the traffic light both for roads ID2 and ID5, while *green color line* represents the estimated density of vehicles on the road according to roads' priorities and this is equivalent to a longer green cycle of the traffic light for road ID2 and shorter for ID5.

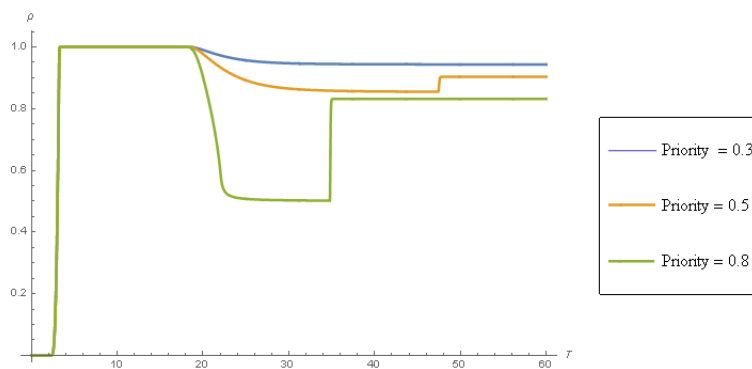


Figure 5.15 Intersection A - Incoming Road ID2 - RS 2 Simulation with different priorities

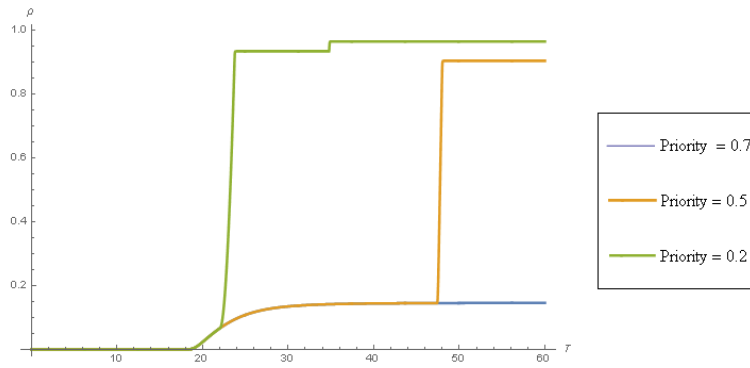


Figure 5.16 Intersection A - Incoming Road ID5 - RS 2 Simulation with different priorities

From both figures it seems obvious as the best solution for reducing congestion state at intersection is the one in which the road ID2 has priority equal to 0.3 and the road ID5 has priority equal to 0.7.

In order to confirm this assumption, it is important to observe and analyze the behaviour of this choice (also compared to others) on the outgoing road of the intersection (i.e. road ID6). Figure 5.17 shows vehicular flow for this road.

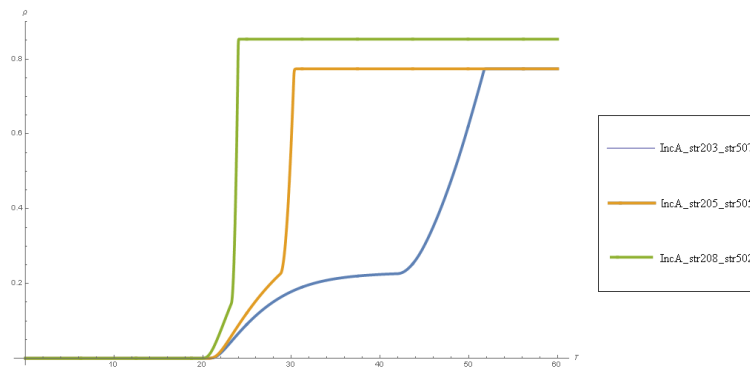


Figure 5.17 Intersection A - Outgoing Road ID6 - RS 2 Simulation with different priorities

Also for outgoing road ID6, the solution considering the pri-

ority for road ID2 equal to 0.3 and for road ID5 equal to 0.7 is the most appropriate because it decrease congestion states at the intersection (in fact car density values are low).

However, we also analyzed the effect of this solution on other roads of the network. As example, Figure 5.18 shows vehicular traffic on the road ID7 that is important because it is the incoming road for intersection C whose one outgoing road is ID5.

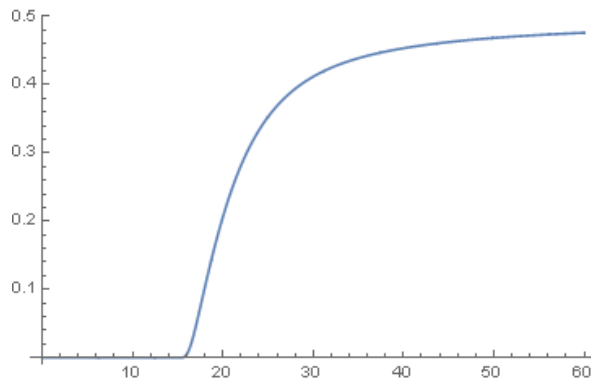


Figure 5.18 Intersection C - Incoming Road ID7 - RS 2 Simulation with $q_2=0.3$ and $q_5=0.7$

As shown in figure, cars density is always less than 0.5 so there are no congestion states on intersection C or, at least, are decreased.

In conclusion, from this set of experimentation activities, we highlighted how the models based on Riemann Solver can be useful for designing an optimal solution to enhancement of driveability on a road network with intersections.

Chapter 6

Conclusions

Analysts, traffic engineers and programmers work together for years to provide a set of information, tools and applications aimed at improving driveability along the entire road network.

This information must be translated into modifications that, though necessary, must be sufficient to meet the costs of management and maintenance of the various authorities responsible for urban roads and not.

Simulation of traffic flows may be helpful in order to identify critical areas and predict traffic evolution due to maintenance works before they are made. Specifically, traffic flux can be optimized by intervening, in some cases, simply on street signs, priority or stop at intersections and on installation of traffic lights, and/or by imposing speed limits on critical areas, therefore avoiding structural and invasive changes to topology of the road network.

In purely application perspective, results obtained by simulation of traffic flows may be useful as support for authorities responsible for urban road network in order to make an appropriate urban planning to the needs of the country, so to avoid traffic congestion at certain areas or time slots and, as a result, bring down the rate of air pollution or noise and minimize risks due to overcrowding of vehicles on roads.

Bibliography

- [1] A. Aw, M. Rascle, *Resurrection of “second order” models of traffic flow?*, SIAM J. Appl. Math., 60:916-938, Elsevier Lt, 2000.
- [2] C. Bardos, A. La Roux, J. Nedelec, *First order quasilinear equations with boundary conditions*, Comm. Partial Differential Equations, 4:1017-1034, 1979.
- [3] N. Bellomo, V. Coscia, *First order models and closure of the mass conservation equation in the mathematical theory of vehicular traffic flow*, C. R. Mec., 333:843-851, 2005.
- [4] S. Benzoni-Gavage, R. M. Colombo, *An n-populations model for traffic flow*, Euro. J. Appl. Math., 14:587-612, 2003.
- [5] S. Blandin, G. Bretti, A. Cutolo, B. Piccoli, *Numerical simulations of traffic data via fluid dynamic approach*, Applied Mathematics and Computation, 210:441-454, 2009.
- [6] N. Cascone, C. D’Apice, B. Piccoli, L. Rarita’, *Optimization of traffic on road networks*, Mathematical Models and Methods in Applied Sciences, 17, 10:1587-1617, 2007.
- [7] Y. Chitour, B. Piccoli, *Traffic circles and timing of traffic lights for cars flow*, Discrete and Continuous Dynamical Systems, B5:599-630, 2005.
- [8] G. Coclite, M. Garavello, B. Piccoli, *Traffic Flow on Road Networks*, SIAM Journal on Mathematical Analysis, 36:1862-1886, 2005.

-
- [9] C. Daganzo, *Requiem for second-order fluid approximation to traffic flow*, Transportation Research, Part B, 29:277-286, Elsevier Lt, 1975.
- [10] C. D'Apice, R. Manzo, B. Piccoli, *Traffic flow on telecommunication networks*, SIAM Journal of Mathematical Analysis, 36:1862-1886, 2006.
- [11] C. D'Apice, B. Piccoli, *Vertex Flow Models for Vehicular Traffic on Networks*, Mathematical Models and Methods in Applied Sciences, 18:1299-1315, 2008.
- [12] C. De Nicola, R. Manzo, V. Moccia, V. Tufano, *Traffic Light Simulation with Time-varying Distribution at Junctions*, 24th European Modeling and Simulation Symposium, 256-264, 2012.
- [13] R. Frattaruolo, R. Manzo, L. Rarita', *Simulation and Optimization of Vehicular Flows in a Harbour*, 20th European Modeling and Simulation Symposium, 638-646, 2008.
- [14] M. Garavello, B. Piccoli, *Traffic Flow on Networks - Conservation Laws Models*, AIMS Series on Applied Mathematics, 1:43-64, American Institute of Mathematical Sciences, 2006.
- [15] M. Garavello, B. Piccoli, *Source-destination flow on road network*, Commun. Math. Sci., 3:261-283, 2005.
- [16] M. Garavello, B. Piccoli, *Traffic flow on a road network using the Aw-Rasclé model*, Commun. Partial Diff. Eqns., 31:243-275, 2006.
- [17] S. K. Godunov, *A finite difference method for the numerical computation of discontinuous solutions of the equations of fluid dynamics*, Mat. Sb., 47:271-290, 1959.
- [18] D. Helbing, *Traffic and related self-driven many-particle systems*, Reviews of Modern Physics, 73:1067-1141, 2001.

-
- [19] M. Herty, C. Kirchner, S. Moutari, *Multi-class traffic models on road networks*, Commun. Math. Sci., 4:591-608, 2006.
- [20] M. Herty, S. Moutari, M. Rascle, *Optimization criteria for modelling intersections of vehicular traffic flow*, Networks and Heterogeneous Media, 1:275-294, 2006.
- [21] A. Marigo, B. Piccoli, *A fluid dynamic model for T-junctions*, SIAM J. Math. Anal., 39(6), 2016-2032, 2008.
- [22] H. J. Payne, *FREFLO: a macroscopic simulation model of freeway traffic*, Transportation Research Record, 722:68-75, 1979.
- [23] H. J. Payne, *Models of freeway traffic and control*, Simulation Council, 10, Simulation Councils Incorporated, 1971.
- [24] K. Pushkin, S. Shankar, *Traffic Flow Theory - Mathematical Framework*, University of California Berkeley, 27-42, Pushkin Kachroo, 2001.
- [25] P. I. Richards, *Shock waves on the highway*, Operations Research, 42-51, Technical Operations, Inc., Arlington, Massachusetts, 1956.
- [26] D. Serre, *Systems of Conservation Laws I and II*, Diderot Editeur, 1996.
- [27] E. B. Setiawan, D. Tarwidi, R. F. Umbara, *Numerical Simulation of Traffic Flow via Fluid Dynamics Approach*, International Journal of Computing and Optimization Vol. 3, 1:93-104, 2016.
- [28] G. B. Whitham, *Linear and Nonlinear Waves*, Pure and Applied Mathematics, 1974.
- [29] G. B. Whitham, M. J. Lighthil, *On kinetic waves. II. Theory of traffic flows on long crowded roads*, Proc. Roy. Soc. London Ser. A, 229:317-345, 1955.

- [30] H. M. Zhang, *A theory of nonequilibrium traffic flow*, Transportation Research, Part B, 32:485-498, 1998.
- [31] H. M. Zhang, *A non-equilibrium traffic model deviod of gas-like behaviour*, Transportation Research, Part B, 36B, 2002.